Contrib Mineral Petrol (2006) 152: 89–110
DOI 10.1007/s00410-006-0096-1

ORIGINAL PAPER

Feiko Kalsbeek · Robert Frei

The Mesoproterozoic Midsommersø dolerites and associated high-silica intrusions, North Greenland: crustal melting, contamination and hydrothermal alteration

Received: 1 August 2005 / Accepted: 27 February 2006 / Published online: 24 May 2006

Abstract The Midsommersø dolerites and the flood basalts of the Zig-Zag Dal Basalt Formation, eastern North Greenland, represent a major Mesoproterozoic (~1,380 Ma) igneous event. The intrusive rocks form large sheets within a succession of feldspathic sandstones which underlie the basalts. The geochemistry of the basalts has recently been re-investigated and reported elsewhere in this Journal; here we present new trace element and Nd-, Sr- and Pb-isotopic data for the intrusive rocks. Unlike the basalts, the intrusions yield evidence of considerable interaction and contamination with upper crustal rocks, especially the sandstones. High-silica rocks (80–90 wt% SiO_2) occur in sheets, up to 60 m thick. They were formed by mobilisation of sandstones, and indicate a very high rate of emplacement of hot basic magma into the sandstones at depth. These mobilised sandstones ('rheopsammites') are among the most SiO_2-rich intrusive rocks on earth. Sheets of remobilised granitoid rocks from the crystalline basement (~70% SiO_2) are also present. Hydrothermal activity, associated with the igneous event, significantly changed the compositions of the silicic rocks as well as that of many dolerites. Sheets of hydrothermally altered ('red') dolerites and silicic rocks invariably have borders of dark, fresh dolerite; this is interpreted to be the result of intrusion from zoned magma chambers. Nd isotope data confirm the crustal origin of the silicic rocks as well as the contamination of some dolerites by components derived from crustal sources, while Sr- and Pb-isotopic systems are strongly affected by the hydrothermal alteration, and give little information on the petrogenesis of the rocks. Recent loss of Sr from hydrothermally altered rocks further affected the Sr isotope systems, and earlier age determinations by the Rb–Sr whole-rock isochron method (1,230 Ma) have proved to be in error. The dolerites and the basalts are geochemically very similar, but most dolerites have moderately negative Eu anomalies that are not observed in the basalts. Eu anomalies in the dolerites could be related to contamination by sandstone at depth, but it is not clear why the basalts escaped a similar contamination.

Communicated by F. Poitrasson

F. Kalsbeek (✉)
Geological Survey of Denmark and Greenland,
Øster Voldgade 10, 1350 Copenhagen K, Denmark
E-mail: fk@geus.dk

R. Frei
Geological Institute, Copenhagen University,
Øster Voldgade 10, 1350 Copenhagen K, Denmark

Introduction

The sandstones of the Independence Fjord Group in eastern North Greenland (around 81°N) are cut by numerous mafic intrusions, known as the Midsommersø dolerites, which are spectacularly exposed along many fjord and valley walls (Fig. 1). Locally more than 75% of the stratigraphy is made up of intrusive rocks, and their cumulative thickness probably far exceeds 1 km. Associated with the dolerites there are large sheets of silicic rocks, up to 60 m wide; some of these contain 80–90 wt% SiO_2 and have been interpreted to represent mobilised sandstones (Jepsen 1971).

The stratigraphy in this part of North Greenland is summarised in Fig. 2. A crystalline basement, hidden below the Inland Ice, is unconformably overlain by the Independence Fjord Group, a succession of Palaeo- to Mesoproterozoic quartzitic and feldspathic sandstones (Collinson 1983). The basement is not exposed in this part of North Greenland, but numerous ice-transported boulders of granitoid rocks are scattered all over the region. The Independence Fjord Group, with its multitude of intrusions, is conformably overlain by an up to ~1,350 m succession of tholeiitic flood basalts, the Zig-Zag Dal Basalt Formation (Kalsbeek and Jepsen 1984; Upton et al. 2005). A genetic relationship between the

Fig. 1 Sandstones of the Independence Fjord Group, eastern North Greenland, with Midsommersø dolerites. Note columnar jointing in some of the large dolerite sheets. Cliff height ~800 m

intrusions and the overlying lavas has always been postulated. The Zig-Zag Dal basalts are unconformably overlain by Neoproterozoic deposits, and the original extent and thickness of the basalts are therefore unknown.

The Midsommersø dolerites and associated silicic intrusions were studied in some detail by Kalsbeek and Jepsen (1983). That study was based on a large number of major element analyses and Rb–Sr isotope data. Only little information on trace element concentrations was available at that time. The main conclusions of that study were that: (1) The rocks comprise a spectrum of compositions, grading from mantle-derived to crustally derived lithologies. (2) Hydrothermal alteration had a profound influence on the compositions of the dolerites and changed their colours from dark grey to red-brown or brick-red. (3) The most silicic intrusions represent remobilised granitoid basement as well as remobilised sandstone (termed 'rheopsammite'); the latter are among the most SiO_2-rich rocks on earth (SiO_2 80–90 wt%). All these silicic rocks have suffered hydrothermal alteration and invariably occur in composite intrusions with borders of dark doleritic rock (Fig. 2 in Kalsbeek and Jepsen 1983). (4) A Rb–Sr whole-rock isochron age of 1,230 ± 20 Ma obtained from a hydrothermally altered 'red' dolerite was thought to date a syn-magmatic hydrothermal event. This age was interpreted indirectly to date the emplacement of the dolerites.

The Zig-Zag Dal basalts and a few samples of Midsommersø dolerites have recently been re-studied by Upton et al. (2005). These authors conclude that the igneous activity was due to melting beneath an attenuating continental lithosphere related to the ascent of a mantle plume. The lavas have been subdivided into three units, the Basal (lower), Aphyric (middle) and Porphyritic (upper) units, and show a gradual upward decrease in Mg number, $MgO/(MgO + Fe_2O_3^T)$. The Porphyritic unit is characterised by notably higher $Fe_2O_3^T$ and TiO_2 than the lower units. A U–Pb baddeleyite date of 1,382 ± 2 Ma, obtained on a dolerite sample from the locality Kap Ejnar Mikkelsen 1, described later in this paper, was taken to represent the age of the lavas and the dolerites. This is 150 million years older than the Rb–Sr whole-rock isochron age obtained by Kalsbeek and Jepsen (1983).

In this paper we present new trace element [including rare earth element (REE)] and isotopic (Sm–Nd, Rb–Sr, Pb–Pb) data, in order to: (1) Test the earlier conclusions

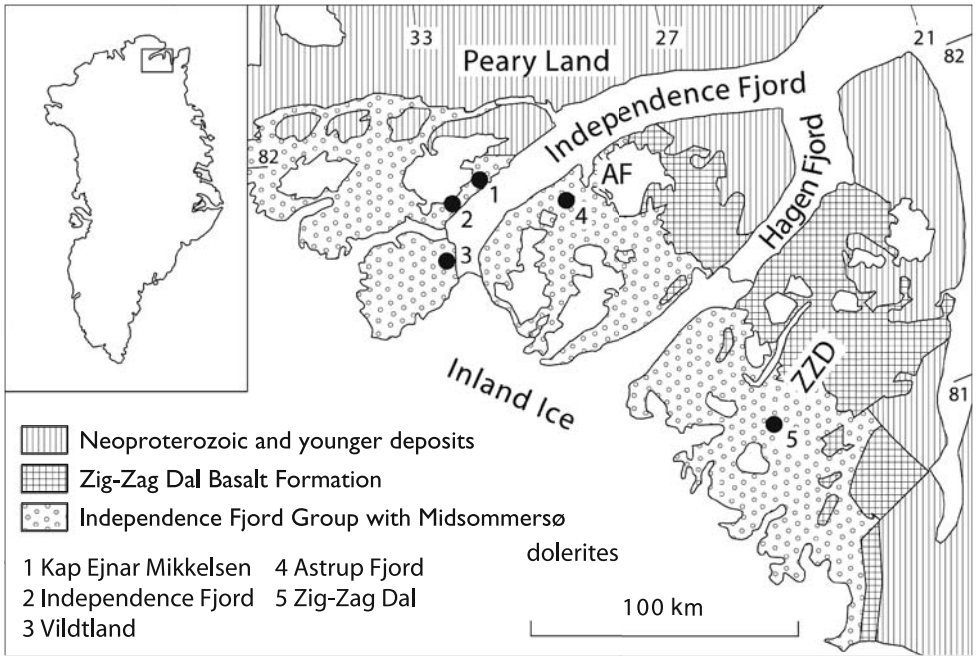

Fig. 2 Geological map showing the distribution of the Independence Fjord Group and the Zig-Zag Dal Basalt Formation in eastern North Greenland, based on the Geological Map of Greenland, 1:2,500,000 (Escher and Pulvertaft 1995); intrusions not shown. *AF* Astrup Fjord, a little branch of Independence Fjord, *ZZD* Zig-Zag Dal. Samples analysed for this study come from the localities 1–5 shown on the map; for precise locations see Appendix

regarding the crustal origins of the silicic rocks and evaluate the conditions under which they were formed. (2) Study the relative roles of crustal contamination and hydrothermal alteration on the compositions of the doleritic rocks, some of which have up to 63 wt% SiO_2. (3) Seek an explanation of the disagreement between the Rb–Sr whole-rock and U–Pb baddeleyite ages of the dolerites. (4) Further compare the chemical and isotopic compositions of the intrusions and the lavas. (5) In general add to the knowledge of this spectacular but, unfortunately, very remote Precambrian igneous province.

Sample selection, petrography and major element compositions

For the present study 29 samples were selected from the larger collection studied previously by Kalsbeek and Jepsen (1983). They come from eight different intrusions: doleritic rocks at Kap Ejnar Mikkelsen, Independence Fjord, Vildtland and Zig-Zag Dal (Fig. 2), granophyric rocks from Kap Ejnar Mikkelsen, and 'rheopsammitic' rocks (rocks containing large proportions of partially melted sandstone) from a locality near Astrup Fjord, from Vildtland, and from Zig-Zag Dal. For information on precise localities and the position of individual samples within each intrusion see Appendix. Since the petrography and major element chemistry of the rocks have been dealt with previously (Kalsbeek and Jepsen 1983), only a brief summary is presented here.

Well-preserved dolerites consist mainly of augite and plagioclase. In some of the samples pigeonite was observed, and pseudomorphs after olivine are present near the base of some intrusions. Minor proportions of biotite and apatite may also be present. As mentioned in the introduction many of the dolerites have undergone severe hydrothermal alteration. While unaltered dolerites are dark grey in colour, the altered rocks are commonly red-brown or brick-red, probably due to the presence of finely disseminated haematite. In hand specimen these rocks appear fresh, but inspection of thin sections reveals that the feldspars are totally replaced by secondary minerals. Fresh augite is commonly present. Some samples have a fine-grained granophyric matrix. Sheets of such 'red dolerites' always have rims, up to several metres wide, of unaltered dark-grey dolerite; the latter are chilled against the sandstones but have gradual transitions towards the red doleritic centres.

Lithologies termed 'granophyric rocks', and 'rheopsammites' have compositions similar to samples from the crystalline basement and sandstones of the Independence Fjord Group, respectively. The granophyric rocks are fine grained and consist mainly of totally altered feldspar and quartz, together with fine-grained secondary minerals. The feldspar (turbid albite) commonly exhibits a 'hollow crystal' habit, indicating rapid crystallisation from a supercooled magma. Granophyric textures are only locally observed, and the term 'granophyric rock' is mainly used because of the lack of a better designation. The matrix locally reveals globules with radial textures, suggesting that parts of the matrix may represent devitrified glass. Rheopsammitic samples are often heterogeneous, containing sandstone fragments representing variable degrees of melting, together with schlieren of granophyric material with some chlorite. More homogeneous samples are also present. Quartz occurs both as pseudomorphs after tridymite, commonly with hollow crystal growth, and as corroded remnants of sedimentary sand grains (Fig. 3).

Major element analyses are available for ~100 samples. In Fig. 4 their compositions are shown in a TAS (total alkalis vs. SiO_2) diagram. The dolerites from the locality denoted Kap Ejnar Mikkelsen 1 have the lowest concentrations of SiO_2 (49–52% on a volatile-free basis) and alkalis (usually 2–2.5% but, due to fractional

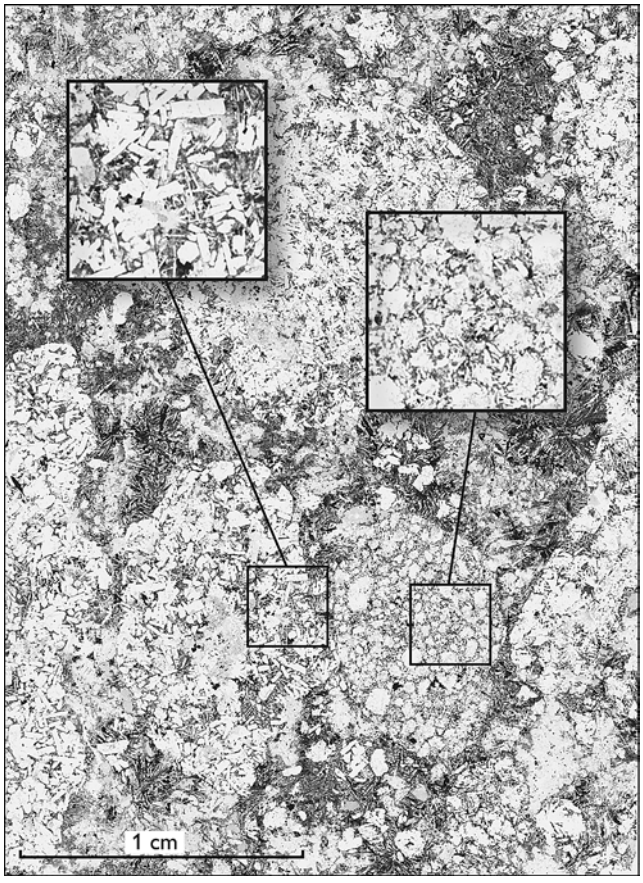

Fig. 3 Inhomogeneous rheopsammite (#197406, Astrup Fjord) at the contact with red granophyric dolerite, consisting of variously transformed sandstone inclusions in a very fine-grained matrix. Translucent crystals are quartz. In one inclusion round corroded detrital quartz grains are preserved (see enlargement), while other inclusions are mainly built up of stubby subhedral grains interpreted as early tridymite, now replaced by quartz (enlargement). Some crystals exhibit a 'hollow crystal' habit (not visible in the photograph), suggesting rapid crystallisation from a supercooled melt. The matrix consists of needle-shaped quartz (after tridymite?), apparently formed during quenching, in a submicroscopic turbid ground mass with chlorite and opaque minerals

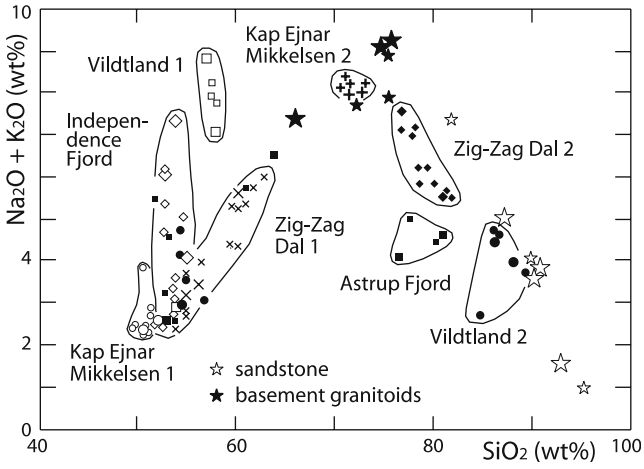

Fig. 4 Total alkalis vs. SiO_2 diagram (wt%, analyses recalculated to 100% on volatile-free basis) for Midsommersø dolerites and associated silicic intrusions; for comparison the compositions of a few samples from the crystalline basement (glacially transported boulders) and the sandstones are also shown. Diagram based on analyses from the study of Kalsbeek and Jepsen (1983); samples selected for the present investigation are shown with somewhat *larger symbols*. The samples are grouped according to individual intrusions, but sheets of silicic rocks (Astrup Fjord, Vildtland 2) have doleritic borders which plot together with other dolerites (Independence Fjord, Zig-Zag Dal 1), outside the field defined by the silicic samples. The same is true for the dark doleritic border of the 'red' $Na_2O + K_2O$-rich dolerite of Vildtland 1

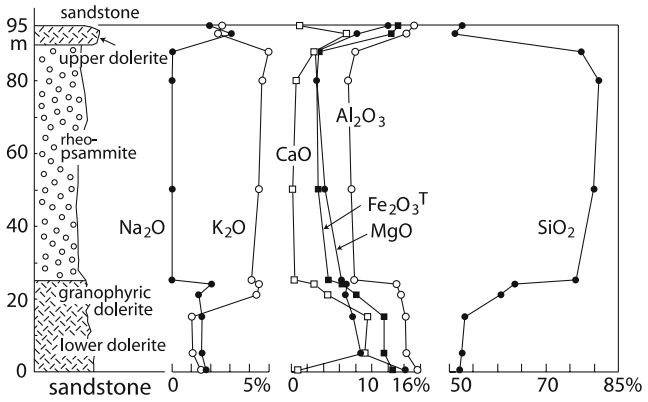

Fig. 5 Chemical variation across the intrusion south of Astrup Fjord. All concentrations in weight percentages after recalculation to 100% volatile-free

crystallisation, up to ~4% in some samples). Most other unaltered doleritic rocks have 52–55% SiO_2 and up to ~3.5% alkalis. Hydrothermally altered 'red' dolerites from the localities Vildtland 1, Independence Fjord and Zig-Zag Dal 1 have much higher proportions of $Na_2O + K_2O$, up to ~9% in samples from the locality Vildtland 1; these samples are depleted in CaO. The high concentrations of SiO_2 in samples from Vildtland 1 and the upper parts of the Zig-Zag Dal 1 intrusion, relative to most other dolerites (Fig. 4), were interpreted by Kalsbeek and Jepsen (1983) as the result of crustal contamination.

The granophyric rocks from the locality Kap Ejnar Mikkelsen 2 plot close to analysed granitoid basement samples in the TAS diagram, and rheopsammitic rocks from Vildtland 2 plot close to some of the sandstones. Samples from the locality Zig-Zag Dal 2 have compositions intermediate between the sandstones and basement samples, and may contain components from both sources. Rare remnants of corroded sand grains are present, and therefore we include them with the rheopsammites. The rheopsammitic rocks from the Astrup Fjord locality are slightly less silicic than those from Vildtland, and may contain some disintegrated doleritic matter. As noted before, all these intrusions have normal doleritic margins which plot together with other dolerites in the TAS diagram.

As a further illustration of the compositional diversity of the rocks, Fig. 5 depicts the variation in chemistry across the intrusion at Astrup Fjord. This intrusion is a ~95 m thick subhorizontal sheet with a central ~65 m thick layer of rheopsammitic rocks. The lower 25 m consist of doleritic rocks that upwards become richer in SiO_2 and K_2O and grade into red granophyric dolerite. At 25 m the rocks change dramatically in chemistry, with very high SiO_2, high K_2O, very little CaO, and virtually no Na_2O in the hydrothermally altered central rheopsammites. The upper ~10 m of the intrusion consist again of dolerite. The chilled dolerites adjacent to the upper and lower sandstones have also been affected by hydrothermal alteration, during which most CaO was lost. Similar variation diagrams for the intrusions Kap Ejnar Mikkelsen 1, Independence Fjord and Vildtland 2 have been presented by Kalsbeek and Jepsen (1983).

The sandstones that host the intrusions consist almost entirely of quartz with variable proportions of K-feldspar (10–45% normative Or in the analysed samples; mean Or = 23.4%). One sample (#273260) has undergone hydrothermal alteration; all feldspar in this sample has been replaced by secondary minerals. Analysed crystalline basement samples (from glacial erratics) have granitic to granodioritic compositions with 10–30% normative Or.

Analytical methods

After jaw crushing the samples (~2 kg) were milled with a Siebtechnik swing mill in a tungsten carbide lined mortar. Most major elements were analysed by X-ray fluorescence spectrometry (XRF) on glass disks at the Geological Survey of Denmark and Greenland (GEUS), Copenhagen. Na_2O was determined by atomic absorption spectrometry and Fe_2O_3 by titration. The proportion of volatiles was calculated from the loss on ignition by correction for the oxidation of FeO to Fe_2O_3; for details see Kystol and Larsen (1999). Trace element concentrations were determined by ICP-MS (inductively coupled plasma mass spectrometry). Samples were dissolved in HF and HNO_3, dried and redissolved in HNO_3

and, after dilution, analysed with a Perkin Elmer ELAN 6100 DRC spectrometer, using international standards (Govindaraju 1994) for calibration. For a comparison of GEUS' analytical results on some standards with published values see Table 1.

Sr, Pb and Nd isotope ratios as well as Sm and Nd concentrations were analysed at the Geological Institute, University of Copenhagen, using a VG Sector 54 IT mass spectrometer. Chemical separation of Sr from whole-rock powders was carried out on conventional cation exchange columns, followed by a clean-up of the Sr fraction over miniature columns using Eichrom SrSpec resin. During analysis the value of 0.1194 for the $^{88}Sr/^{86}Sr$ ratio was used for on-line mass fractionation correction, using the exponential bias law. The mean $^{87}Sr/^{86}Sr$ value of the NBS 987 Sr standard was 0.710239, with an external reproducibility of 0.000009 (2σ, $N = 5$) during the analysis time of this project. $^{87}Rb/^{86}Sr$ values ($\pm 2\%$, 2σ) are based on precise Rb/Sr ratios determined by XRF on powder tablets, and calibrated with the help of international standards (Pankhurst and O'Nions 1973).

Pb was separated on conventional anion exchange columns with HBr–HCl, followed by a clean-up on 200 µl Teflon columns. Fractionation of Pb during mass-spectrometric analysis was monitored by repeated analysis of the NBS 981 standard (Todt et al. 1993) and amounted to $0.105 \pm 0.008\%$/amu (2σ, $N = 5$).

For Sm–Nd analysis the rock powders were spiked with a ^{149}Sm–^{150}Nd mixed spike and the bulk REEs were separated over 15 ml glass stem columns charged with AG 50W cation resin. REEs were further separated over HDEHP-coated bio beads (BioRad*) loaded in 6 ml glass stem columns. During analysis both static and multi-dynamic routines were used for the collection of the isotopic ratios. Nd isotope ratios were normalised to $^{146}Nd/^{144}Nd = 0.7219$. The mean value of $^{143}Nd/^{144}Nd$ for our internal JM Nd standard (referenced against La Jolla) during the period of measurement was 0.511109 ± 0.000011 (2σ, $N = 4$). The precision of $^{147}Sm/^{144}Nd$ is better than 2% (2σ).

Decay constants, etc. used in the calculations follow Steiger and Jäger (1977); the age of the earth was assumed to be 4.55 Ga. Sample numbers refer to the files

Table 1 Geological Survey of Denmark and Greenland analytical results on various standards compared to accepted values

Element, isotope	Disko-1			BHVO-2			BIR-1			DNC-1			GA		
Sc 45	37.2	42.6	**40.2**	28.4	32.0	**32**	43.4	41.1	**44**	31.6	28.8	**31**	7.19	6.33	**7**
V 51	399	419	**405**	308	313	**317**	324	311	**313**	154	139	**148**	37.8	33.4	**38**
Cr 52	123	126	**128**	283	288	**280**	389	378	**382**	292	272	**285**	7.20	6.10	**12**
Co 59	56.5	56.5	**54.4**	44.2	44.1	**45**	52.6	51.7	**51**	55.5	54.4	**54.7**	4.83	4.31	**5**
Ni 60	59.2	59.7	**67.0**	117	118	**119**	169	167	**166**	258	248	**247**	4.58	4.29	**7**
Cu 63	230	234	**221**	131	130	**127**	121	118	**126**	96	92	**96**	20.3	17.7	**16**
Zn 66	104	105	**102**	104	104	**103**	67.3	64.9	**71**	60.0	57.9	**66**	64.7	59.2	**80**
Ga 71	21.4	21.1	**20.2**	21.6	21.3	**21.7**	15.5	15.0	**16**	13.7	13.6	**15**	16.6	16.0	**16**
Rb 85	3.37	3.39	**3.22**	9.13	9.05	**9.48**	0.20	0.19	**0.25**	3.59	3.55	**4.5**	170	170	**175**
Sr 88	216	214	**207**	398	384	**399**	108	107	**108**	144	140	**145**	297	294	**310**
Y 89	33.4	33.9	**33.0**	26.7	26.4	**28.3**	16.0	15.9	**16**	18.0	18.0	**18**	21.1	21.0	**21**
Zr 90	125	126	**117**	178	177	**178**	15.2	15.1	**15.5**	37.8	36.9	**41**	102	81	**150**
Nb 93	4.52	4.61	**4.48**	19.2	19.1	**19**	0.56	0.56	**0.6**	1.56	1.56	**3**	12.6	12.8	**12**
Cs 133	0.05	0.06	**0.06**	0.08	0.09		0.01	0.00	**0.01**	0.18	0.19	**0.34**	5.30	5.90	**6.0**
Ba 137	49.2	48.9	**47.5**	131	135	**135**	6.86	6.41	**7**	108	110	**114**	843	871	**840**
La 139	6.47	6.50	**6.49**	15.0	14.9	**15.2**	0.61	0.63	**0.62**	3.71	3.64	**3.8**	42.5	39.2	**40**
Ce 140	16.9	17.4	**17.2**	35.5	36.2	**34.8**	1.87	1.89	**1.95**	7.96	8.00	**10.6**	78.8	74.1	**76**
Pr 141	2.96	2.93	**2.90**	5.62	5.58	**5.57**	0.38	0.38	**0.38**	1.15	1.12	**1.3**	9.31	8.56	**8.3**
Nd 143	14.8	14.9	**14.9**	25.2	25.1	**24.9**	2.43	2.41	**2.5**	5.03	4.88	**4.9**	31.1	28.8	**27**
Sm 147	4.56	4.64	**4.59**	5.92	6.18	**6.16**	1.06	1.08	**1.1**	1.39	1.40	**1.38**	5.20	5.01	**5**
Eu 153	1.71	1.66	**1.58**	2.09	2.05	**2.03**	0.53	0.52	**0.54**	0.58	0.56	**0.59**	1.01	0.98	**1.08**
Gd 157	5.66	5.74	**5.87**	6.56	6.77	**6.13**	1.71	1.72	**1.85**	2.06	2.05	**2**	5.53	5.35	**3.8**
Tb 159	0.99	0.98	**0.99**	0.98	0.99	**0.96**	0.36	0.35	**0.36**	0.40	0.39	**0.41**	0.67	0.67	**0.6**
Dy 161	5.92	6.03	**5.90**	5.31	5.33	**5.3**	2.52	2.40	**2.5**	2.72	2.64	**2.7**	3.65	3.71	3.3
Ho 165	1.21	1.24	**1.20**	0.99	0.97	**1.01**	0.57	0.57	**0.57**	0.63	0.63	**0.62**	0.68	0.70	**0.7**
Er 166	3.28	3.26	**3.13**	2.53	2.53	**2.5**	1.62	1.56	**1.7**	1.86	1.84	**2**	2.03	2.00	**1.9**
Tm 169	0.50	0.49	**0.49**	0.35	0.35	**0.35**	0.27	0.27	**0.26**	0.30	0.30	**0.33**	0.31	0.32	**0.3**
Yb 174	2.90	2.95	**2.83**	1.98	2.03	**2.05**	1.65	1.61	**1.65**	1.96	1.91	**2.01**	2.04	1.97	**2**
Lu 175	0.44	0.45	**0.45**	0.29	0.30	**0.29**	0.26	0.25	**0.26**	0.31	0.31	**0.32**	0.32	0.31	**0.3**
Hf 177	3.30	3.28	**3.14**	4.39	4.55	**4.42**	0.58	0.56	**0.6**	1.01	0.95	**1.01**	2.96	2.39	**4**
Ta 181	0.31	0.30	**0.30**	1.19	1.19	**1.22**	0.04	0.04	**0.04**	0.09	0.09	**0.10**	1.27	1.30	**1.3**
Pb 208	1.27	1.15	**1.18**	1.49	1.74	**1.53**	2.94	3.00	**3**	7.48	6.28	**6.3**	29.3	30.1	**30**
Th 232	0.58	0.59	**0.60**	1.16	1.18	**1.3**	0.03	0.03	**0.03**	0.24	0.24	**0.2**	16.7	15.8	**17**
U 238	0.15	0.15	**0.14**	0.38	0.42	**0.45**	0.01	0.01	**0.01**	0.06	0.06	**0.1**	5.55	4.75	**5**

All concentrations in ppm; accepted values (Govindaraju 1994) in bold. Disko 1, a basalt from Disko island, West Greenland is GEUS' in-house standard; in this case analytical results obtained at the University of Durham (UK) are used as 'accepted values'

Table 2 Chemical analyses of Midsommersø dolerites and associated rocks

Sample no.	273241	273247	273228	273230	273236	273390	273392	273398	273482	273487	273495	273214	273219	197402	197405	197406	197408
	Kap Ejnar Mikkelsen 1		Independence Fjord			Vildtland 1			Zig-Zag Dal 1			Kap Ejnar Mikkelsen 2		Astrup Fjord			
SiO_2 (%)	49.57	51.18	53.24	50.52	50.55	52.44	55.71	55.42	53.75	54.21	58.82	68.98	69.56	51.41	60.15	73.55	78.67
TiO_2	1.17	1.20	1.06	0.90	1.00	0.94	0.81	0.80	0.80	0.63	0.56	0.37	0.41	0.96	0.50	0.35	0.24
Al_2O_3	14.15	14.28	14.18	15.35	15.40	13.58	12.83	13.50	14.27	12.46	13.59	12.79	12.31	13.93	12.39	7.54	6.91
Fe_2O_3	3.99	3.12	3.16	2.99	3.00	2.59	2.53	3.27	2.71	2.40	2.17	0.78	1.85	4.06	2.33	2.49	1.61
FeO	8.81	9.53	7.27	6.17	5.78	7.36	5.74	4.97	6.36	5.75	4.22	2.14	1.42	6.46	3.32	1.77	1.36
MnO	0.24	0.24	0.20	0.19	0.11	0.21	0.19	0.11	0.13	0.12	0.09	0.11	0.08	0.14	0.11	0.07	0.04
MgO	8.17	6.09	5.36	7.83	10.56	7.06	5.99	6.25	6.98	7.95	5.03	2.92	2.59	8.41	6.57	5.99	3.10
CaO	10.06	10.40	8.55	5.93	0.52	9.72	5.48	4.10	9.57	9.59	7.13	0.29	0.23	8.95	2.69	0.40	0.61
Na_2O	1.92	2.30	2.24	3.75	0.61	1.83	3.01	1.82	1.60	1.75	2.72	2.93	2.97	1.49	1.91	0.01	0.00
K_2O	0.38	0.27	1.75	2.12	6.26	0.97	3.78	6.74	1.49	1.58	2.77	4.91	4.75	1.04	4.29	3.95	4.51
P_2O_5	0.10	0.11	0.16	0.11	0.14	0.12	0.10	0.11	0.09	0.08	0.08	0.10	0.09	0.09	0.05	0.05	0.05
Volat.	1.46	1.43	2.35	3.57	5.73	1.95	2.47	2.44	1.80	2.82	2.29	2.02	1.69	2.63	4.96	3.04	2.13
Sum	100.02	100.15	99.52	99.43	99.66	98.77	98.64	99.53	99.55	99.34	99.47	98.34	97.95	99.57	99.27	99.21	99.23
Cs (ppm)	0.31	0.07	0.21	0.78	1.51	0.81	0.45	0.59	0.23	0.26	0.75	0.95	0.93	1.55	0.70	0.22	0.17
Rb	8.0	4.90	42	58	66	27	69	72	37	44	79	109	114	29	135	88	85
Ba	132	116	333	435	500	277	492	335	313	270	408	1050	874	237	568	492	453
Pb	1.44	1.43	7.4	6.1	46	6.5	11.3	9.9	5.3	4.44	11.9	27	12.9	7.1	9.9	7.0	4.42
Sr	151	177	222	196	60	171	155	56	173	153	139	101	74	150	78	18.4	10.6
Y	24	26	31	24	31	30	29	30	25	19.8	18.6	15.4	22	25	14.0	10.5	10.1
Th	0.68	0.73	3.66	2.21	3.73	3.09	4.67	4.67	3.28	2.52	2.87	12.1	13.0	1.74	2.44	3.00	4.44
U	0.18	0.17	0.99	0.64	1.08	0.82	1.25	1.31	0.91	0.69	0.76	3.04	3.05	0.43	0.56	0.59	1.00
Zr	79	86	157	121	169	150	187	193	113	89	100	168	224	91	83	85	108
Hf	2.08	2.26	3.85	2.91	3.86	3.54	4.59	4.51	2.87	2.34	2.51	4.29	5.53	2.39	2.14	2.22	2.84
Nb	3.80	3.82	13.2	9.3	13.7	11.7	11.4	11.7	9.9	7.1	7.0	11.3	12.2	5.0	3.61	2.83	2.93
Zn	92	92	82	54	175	73	73	74	67	57	48	43	41	76	70	56	33
Cu	177	182	104	80	245	98	80	76	84	61	59	143	3.97	129	88	81	47
Ni	161	58	43	62	56	60	53	50	83	132	74	21	17.9	100	59	24	17.4
Sc	38	43	35	37	40	32	27	25	32	36	27	7.5	8.1	36	24	12.6	8.3
V	349	349	273	249	267	239	198	184	226	186	164	51	54	301	154	95	62
Cr	102	24	26	321	140	124	128	108	224	442	120	48	42	97	97	21	24
Ga	18.1	19.3	17.1	15.1	17.7	16.8	16.7	16.4	15.6	13.2	13.3	17.6	18.1	16.7	12.2	9.0	7.5
La (ppm)	6.79	7.29	23.6	16.3	25.5	21.4	25.2	26.1	16.7	13.7	14.7	33.2	42.2	10.1	11.5	9.30	9.83
Ce	15.6	16.6	48.6	34.0	53.7	44.8	50.4	53.0	33.8	27.8	30.1	65.6	81.5	21.5	22.1	19.8	21.1
Pr	2.34	2.45	6.39	4.28	6.51	5.82	6.77	6.61	4.57	3.35	3.59	7.58	9.46	3.06	2.85	2.46	2.64
Nd	10.7	11.1	24.3	16.9	25.1	22.3	25.1	24.6	17.2	12.9	13.6	26.1	33.6	12.6	11.0	8.81	9.16
Sm	2.93	3.10	4.96	3.58	5.27	4.53	4.83	4.93	3.64	2.74	2.76	4.29	5.52	3.10	2.21	1.68	1.57
Eu	1.05	1.13	1.31	0.97	1.22	1.16	1.13	1.10	1.00	0.76	0.76	0.89	0.98	0.95	0.63	0.32	0.30
Gd	3.68	3.96	5.77	4.39	6.20	5.55	5.75	5.82	4.33	3.42	3.39	4.69	5.99	3.94	2.75	2.02	1.96
Tb	0.64	0.68	0.88	0.67	0.92	0.84	0.83	0.83	0.66	0.52	0.51	0.53	0.74	0.67	0.39	0.29	0.27
Dy	4.03	4.34	5.25	4.06	5.50	5.00	5.00	4.97	4.12	3.11	2.97	2.79	3.97	4.10	2.40	1.79	1.64
Ho	0.88	0.94	1.11	0.84	1.12	1.03	1.05	1.01	0.88	0.67	0.64	0.49	0.75	0.89	0.50	0.38	0.36
Er	2.41	2.55	3.20	2.44	3.21	2.92	2.97	2.93	2.53	1.96	1.84	1.39	2.10	2.51	1.46	1.14	1.13
Tm	0.38	0.42	0.50	0.38	0.51	0.47	0.46	0.46	0.40	0.32	0.29	0.19	0.32	0.38	0.22	0.19	0.18
Yb	2.38	2.48	3.19	2.38	3.11	2.84	2.90	2.83	2.49	1.91	1.83	1.22	1.94	2.39	1.43	1.14	1.20
Lu	0.37	0.41	0.48	0.38	0.51	0.45	0.45	0.45	0.38	0.31	0.30	0.19	0.30	0.36	0.23	0.18	0.19

Table 2 (Contd.)

Sample no.	273364	273367	273370	273525	273532	197429	197439	197440	273260	273262	273293	273402
	Vildtland 2			Zig-Zag Dal 2		Crystalline basement			Sandstones			
SiO_2 (%)	52.62	87.31	85.32	79.81	75.30	64.08	73.61	72.66	91.97	86.46	90.20	89.92
TiO_2	0.86	0.08	0.11	0.27	0.37	0.49	0.06	0.20	0.06	0.05	0.04	0.04
Al_2O_3	13.29	5.34	6.11	9.10	10.41	15.16	13.05	13.24	4.74	6.34	4.60	4.89
Fe_2O_3	2.41	0.12	0.09	0.43	1.35	1.01	0.13	0.46	0.02	0.26	0.05	0.21
FeO	6.95	0.76	0.81	1.27	1.09	2.92	0.57	0.94	0.30	0.58	0.28	0.56
MnO	0.18	0.01	0.02	0.02	0.04	0.09	0.03	0.04	0.00	0.00	0.00	0.00
MgO	7.82	1.31	1.65	1.49	1.74	2.12	0.35	0.56	0.15	0.13	0.15	0.07
CaO	9.77	0.10	0.13	0.27	0.15	3.83	0.39	0.30	0.13	0.15	0.05	0.02
Na_2O	1.80	0.31	0.24	1.18	0.10	4.33	3.83	3.69	0.00	0.03	0.01	0.06
K_2O	1.10	3.63	4.20	4.23	7.30	2.82	5.20	5.13	1.55	4.98	3.77	3.55
P_2O_5	0.11	0.04	0.05	0.08	0.08	0.18	0.02	0.05	0.06	0.04	0.03	0.01
Volat.	1.91	0.81	0.99	1.35	1.46	1.02	0.67	0.88	0.83	0.52	0.28	0.58
Sum	98.82	99.82	99.72	99.50	99.39	98.05	97.91	98.15	99.81	99.54	99.46	99.91
Cs (ppm)	1.62	0.19	0.14	0.45	0.41	2.40	1.82	1.68	0.39	1.10	0.85	0.95
Rb	38	80	86	101	120	130	246	285	47	135	106	109
Ba	278	425	450	762	1075	999	510	732	133	718	579	485
Pb	6.65	3.63	2.43	10.6	7.9	19.3	44	24	3.52	13.9	14.7	11.7
Sr	147	18.1	19.7	55	34	507	106	84	6.7	40	32	31
Y	27	8.4	10.8	15.0	23	16.4	21	15.4	4.21	5.4	7.1	7.1
Th	3.36	4.24	5.3	9.1	11.6	18.5	24	43	4.44	3.15	4.25	3.69
U	0.92	0.93	1.09	1.77	1.92	1.30	6.2	2.79	0.82	0.54	0.61	0.71
Zr	141	91	118	164	209	226	117	196	65	60	79	52
Hf	3.35	2.35	3.15	4.15	5.4	5.4	4.15	5.6	1.84	1.63	2.24	1.41
Nb	10.5	1.49	2.77	5.1	7.4	6.9	6.7	15.5	1.87	0.98	1.47	1.88
Zn	69	8.9	12.8	15.0	32	55	13.3	16.6	2.72	4.23	1.83	2.61
Cu	102	5.1	4.95	10.7	1.12	13.5	1.20	1.72	20	3.38	1.56	1.09
Ni	80	6.3	8.6	13.8	9.2	26	1.08	1.98	1.77	1.58	1.60	1.74
Sc	33	2.00	2.77	5.1	6.3	8.5	1.49	2.22	0.90	0.94	0.81	0.84
V	236	10.5	12.2	31	29	64	4.45	9.2	6.1	6.2	2.75	4.16
Cr	257	12.3	21	33	24	41	1.75	3.07	3.34	2.98	3.51	2.95
Ga	16.3	4.61	5.8	10.5	12.7	21	21	25	3.89	5.9	4.21	4.97
La (ppm)	19.6	9.39	14.6	25.0	25.8	59.1	29.8	62.5	7.98	5.60	10.7	6.45
Ce	40.7	19.2	29.2	48.1	50.3	109	55.9	117	17.4	11.2	20.0	12.9
Pr	5.29	2.38	3.58	6.10	6.52	12.3	6.59	13.4	2.00	1.38	2.41	1.66
Nd	20.3	8.42	12.4	20.8	22.8	41.3	20.9	41.9	7.03	5.06	8.37	6.05
Sm	4.26	1.61	2.20	3.51	4.12	6.02	3.90	6.11	1.15	0.97	1.42	1.22
Eu	1.08	0.30	0.42	0.74	0.81	1.16	0.38	0.56	0.21	0.22	0.26	0.27
Gd	5.19	1.83	2.41	3.75	4.79	6.45	4.07	6.23	1.21	1.07	1.51	1.31

Table 2 (Contd.)

Sample no.	273364 Vildtland 2	273367	273370	273525 Zig-Zag Dal 2	273532	197429 Crystalline basement	197439	197440	273260 Sandstones	273262	273293	273402
Tb	0.77	0.24	0.31	0.47	0.69	0.64	0.55	0.66	0.15	0.15	0.21	0.20
Dy	4.67	1.38	1.80	2.61	3.97	3.13	3.16	3.19	0.75	0.90	1.23	1.22
Ho	1.01	0.28	0.36	0.51	0.78	0.53	0.63	0.52	0.14	0.18	0.25	0.25
Er	2.78	0.80	1.07	1.51	2.31	1.58	2.02	1.46	0.42	0.54	0.78	0.73
Tm	0.43	0.13	0.17	0.23	0.35	0.24	0.35	0.20	0.06	0.09	0.14	0.12
Yb	2.63	0.80	1.08	1.49	2.15	1.43	2.34	1.23	0.42	0.56	0.83	0.75
Lu	0.41	0.13	0.17	0.23	0.33	0.21	0.38	0.18	0.07	0.09	0.13	0.12

Sample numbers refer to the files of the Geological Survey of Greenland, now incorporated in the Geological Survey of Denmark and Greenland (GEUS). Samples analysed at GEUS. Most major elements by X-ray fluorescence spectrometry on glass discs; Na_2O by AAS, FeO by titration. Volat. = loss on ignition corrected for the oxidation of FeO to Fe_2O_3 during ignition; see Kystol and Larsen (1999). Trace elements by inductively coupled plasma mass spectrometry, see Sect. 'Analytical methods'

of the former Geological Survey of Greenland, now incorporated into GEUS.

Results

Trace elements

Major and trace element concentrations for the 29 samples selected for this study are given in Table 2. Chondrite-normalised (Taylor and McLennan 1985) REE diagrams for the different intrusions are shown in Fig. 6. Well preserved as well as hydrothermally altered dolerites from Independence Fjord, Vildtland 1 and Zig-Zag Dal 1 have similar REE patterns, with La 37–70 times and Lu 8–13 times chondritic values, La_N/Lu_N 4.6–6.0, and moderately negative Eu anomalies. The grey band in Fig. 6 encompasses the REE data for these three intrusions and is shown for comparison in all diagrams. Gd could not be determined precisely, probably because of minor interference with molecules of ^{138}Ba ^{19}F in Ba-rich samples (Table 1), and Gd concentrations were approximated by interpolation between Sm and Tb in the chondrite-normalised diagrams.

Compared to the other dolerites the two samples from Kap Ejnar Mikkelsen 1 have much flatter REE patterns (La ~20×, Lu ~10× chondrites, La_N/Lu_N 1.8 and 1.9) without a Eu anomaly. Whereas the doleritic border of the rheopsammitic sill Vildtland 2 (#273364) has REE concentrations similar to most other dolerites, the border sample of the Astrup Fjord intrusion (#197402) exhibits a REE spectrum intermediate between samples from Kap Ejnar Mikkelsen 1 and the other dolerites (La_N/Lu_N 2.9, and a small Eu anomaly).

The three granitoid samples from the crystalline basement show variable REE patterns; two have light REE (LREE) higher and heavy REE (HREE) lower than the dolerites, whereas the third sample has LREE and HREE similar to the dolerites. La_N/Lu_N varies from 8 to 29, and all three samples have pronounced Eu anomalies. The two granophyric samples from Kap Ejnar Mikkelsen 2 have REE characteristics somewhat similar to those of the basement samples: higher LREE and lower HREE than the dolerites, La_N/Lu_N 14.5 and 18.1, and marked negative Eu anomalies.

Because of their high proportions of quartz the analysed sandstones have low concentrations of REE (Σ REE 33–48 ppm, compared to 54 and 57 ppm for the dolerites from Kap Ejnar Mikkelsen, and 70–140 ppm for the other dolerites). The sandstones have moderately steep REE patterns, La_N/Lu_N 5.7–12.1, and distinctly negative Eu anomalies. Rheopsammitic rocks from Vildtland 2 (La_N/Lu_N 7.5 and 8.9) have REE patterns similar to those of the sandstones. Rheopsammites from Astrup Fjord (La_N/Lu_N 5.4) also have lower REE (especially HREE) than most of the dolerites, but not as low as the sandstones. REE patterns for the two rheopsammitic samples from Zig-Zag Dal 2 are similar

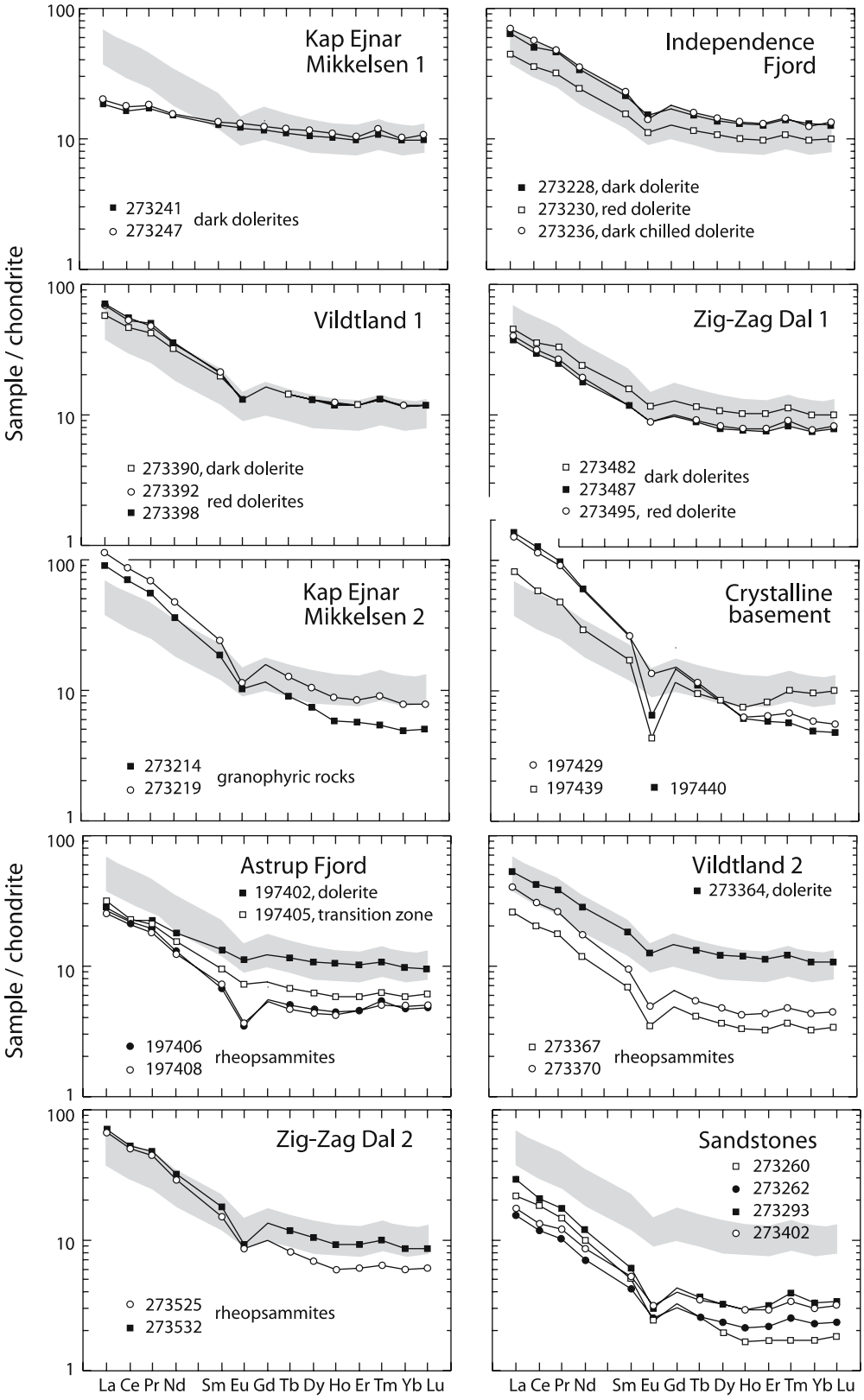

Fig. 6 Chondrite-normalised rare earth element (REE) diagrams for the different intrusions; normalisation values from Taylor and McLellan (1985). The grey band comprises the normalised REE compositions of the dolerites from Independence Fjord, Vildtland 1 and Zig-Zag Dal 1 for comparison with those of the other rocks

to those of the granophyric rocks from Kap Ejnar Mikkelsen 2, but they have slightly lower LREE and, accordingly, slightly lower La_N/Lu_N (8.1 and 11.4, compared to 14.5 and 18.1).

Chondrite-normalised (Thompson 1982) incompatible element spider diagrams for the different intrusions are shown in Fig. 7. Superimposed on a regular downwards slope towards the more compatible elements, most

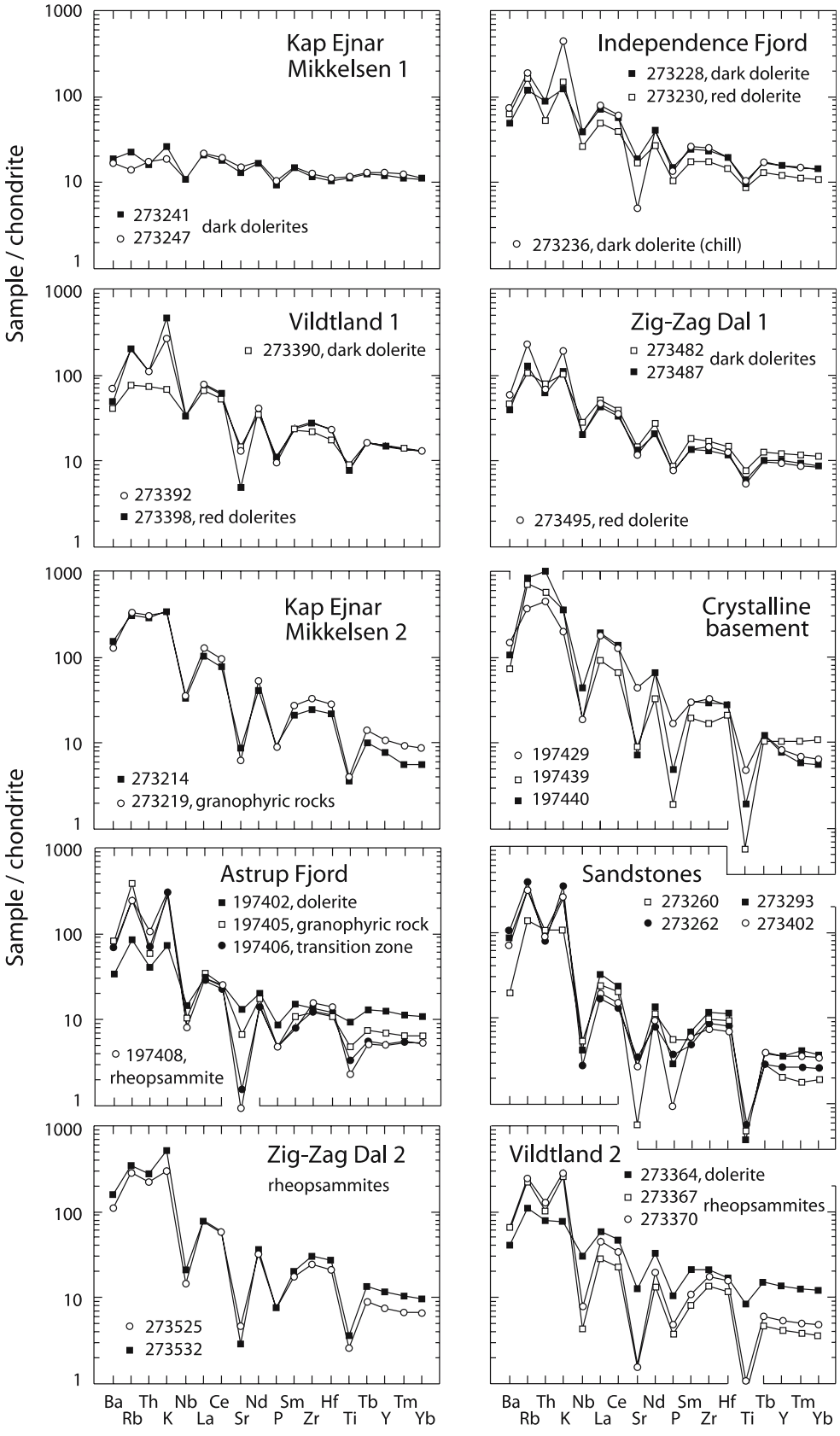

Fig. 7 Chondrite-normalised incompatible trace element diagrams; normalisation values from Thompson (1982)

diagrams show distinct but variable negative anomalies for Nb, Sr, P and Ti (Ta was not used because of contamination during milling in tungsten carbide). Low Ba, and high Rb and K (relative to Th) is apparent in most hydrothermally altered samples. Some of the red dolerites also have much lower Sr than unaltered dolerites.

Samples from the crystalline basement and the sandstones exhibit pronounced negative anomalies for Nb, Sr, P and Ti. Such anomalies are also found for the granophyric rocks of Kap Ejnar Mikkelsen 2, and for the rheopsammites of Vildtland 2, Astrup Fjord and Zig-Zag Dal 2.

Nd isotopes

Sm–Nd isotope data are listed in Table 3. εNd_i values (at 1,382 Ma) are around 0 for the two samples from the dolerite at Kap Ejnar Mikkelsen, and −3 to −5 for the other dolerites (Fig. 8a). There is a statistically significant decrease in epsilon values with increasing proportions of SiO_2. These data are similar to figures obtained for the Zig-Zag Dal basalts by Upton et al. (2005). Samples from the Porphyritic unit have εNd_i from −1 to +1, while the lavas from the Basal and Aphyric units have εNd_i −2 to −4. These authors also report Sm–Nd data on a few Midsommersø dolerites. A sample from the Kap Ejnar Mikkelsen 1 dolerite (#273251) yielded $\varepsilon Nd_i + 0.5$, a sample from Astrup Fjord (#197402—also one of our samples) gave εNd_i − 2.8, and a sample from Zig-Zag Dal 1 (#273493) with 62.6% SiO_2 (volatile-free) had εNd_i − 5.2.

The two rheopsammitic samples from Vildtland 2 have εNd_i values around −10, similar to the sandstones (Fig. 8b), and the two granophyric rocks from Kap Ejnar Mikkelsen 2 have εNd_i around −18, similar to two of the three basement samples. Rheopsammitic samples from Astrup Fjord have εNd_i and SiO_2 intermediate between sandstones and dolerites, and the two samples from Zig-Zag Dal 2 have εNd_i and SiO_2 intermediate between sandstones and basement samples.

Table 3 Sm–Nd isotope data

	Sm (ppm)	Nd (ppm)	$^{147}Sm/^{144}Nd$	$^{143}Nd/^{144}Nd$	$\pm 2\sigma$ (ppm)	T_{CHUR} (Ga)	T_{DM} (Ga) DePaolo	εNd (T = 0)	εNd_i 1,382 Ma
Kap Ejnar Mikkelsen 1									
273241	2.83	10.2	0.1679	0.512391	7	1.30	2.53	−4.8	0.3 ± 0.6
273247	3.13	11.1	0.1707	0.512377	7	1.53	2.75	−5.1	−0.5 ± 0.6
Independence Fjord									
273228	4.82	23.3	0.1254	0.511811	6	1.76	2.32	−16.1	−3.5 ± 0.4
273230	3.62	17.1	0.1285	0.511878	9	1.69	2.28	−14.8	−2.7 ± 0.5
273236	5.38	25.7	0.1267	0.511797	5	1.82	2.38	−16.4	−4.0 ± 0.5
Vildtland 1									
273390	4.48	21.5	0.1263	0.511829	8	1.75	2.31	−15.8	−3.3 ± 0.5
273392	4.71	23.6	0.1207	0.511728	7	1.82	2.34	−17.8	−4.3 ± 0.4
273398	4.78	24.0	0.1203	0.511717	10	1.83	2.35	−18.0	−4.4 ± 0.4
Zig-Zag Dal 1									
273482	3.45	16.4	0.1269	0.511805	9	1.81	2.37	−16.3	−3.9 ± 0.5
273487	2.80	13.2	0.1286	0.511812	8	1.85	2.41	−16.1	−4.1 ± 0.5
273495	2.76	13.5	0.1241	0.511714	9	1.94	2.45	−18.0	−5.2 ± 0.4
Kap Ejnar Mikkelsen 2									
273214	4.34	26.0	0.1009	0.510862	6	2.81	3.11	−34.6	−17.7 ± 0.4
273219	5.58	33.0	0.1024	0.510933	17	2.74	3.05	−33.3	−16.6 ± 0.4
Astrup Fjord									
197402	3.03	12.1	0.1520	0.512083	7	1.89	2.64	−10.8	−2.9 ± 0.5
197405	2.13	10.4	0.1238	0.511716	16	1.92	2.44	−18.0	−5.1 ± 0.4
197406	1.66	8.6	0.1167	0.511588	7	1.99	2.46	−20.5	−6.3 ± 0.4
197408	1.51	8.6	0.1055	0.511383	9	2.09	2.50	−24.5	−8.4 ± 0.4
Vildtland 2									
273364	4.09	19.3	0.1278	0.511834	8	1.77	2.34	−15.7	−3.5 ± 0.5
273367	1.63	8.3	0.1181	0.511360	6	2.47	2.87	−24.9	−11.0 ± 0.4
273370	2.07	11.8	0.1063	0.511302	8	2.24	2.63	−26.1	−10.1 ± 0.4
Zig-Zag Dal 2									
273525	3.40	20.0	0.1030	0.511136	7	2.43	2.78	−29.3	−12.6 ± 0.4
273532	3.91	21.2	0.1117	0.511121	10	2.70	3.04	−29.6	−14.6 ± 0.4
Crystalline basement									
197429	5.97	39.7	0.0911	0.510712	10	2.76	3.04	−37.6	−18.9 ± 0.3
197439	3.55	18.8	0.1144	0.510960	9	3.09	3.38	−32.7	−18.2 ± 0.4
197440	5.93	39.9	0.0900	0.510511	11	3.02	3.26	−41.5	−22.7 ± 0.3
Sandstones									
273260	1.13	6.6	0.1033	0.511236	12	2.28	2.65	−27.4	−10.8 ± 0.4
273262	0.95	4.9	0.1179	0.511401	11	2.38	2.79	−24.1	−10.2 ± 0.4
273293	1.39	8.0	0.1058	0.511273	9	2.28	2.66	−26.6	−10.6 ± 0.4
	1.11	5.7	0.1186	0.511406	8	2.39	2.81	−24.0	−10.2 ± 0.4

Analysed at the Geological Institute, University of Copenhagen. T_{DM} values according to the model of DePaolo (1981). Precisions (2σ) of εNd_i values are based on errors of 2% on $^{147}Sm/^{144}Nd$ ratios (2σ)

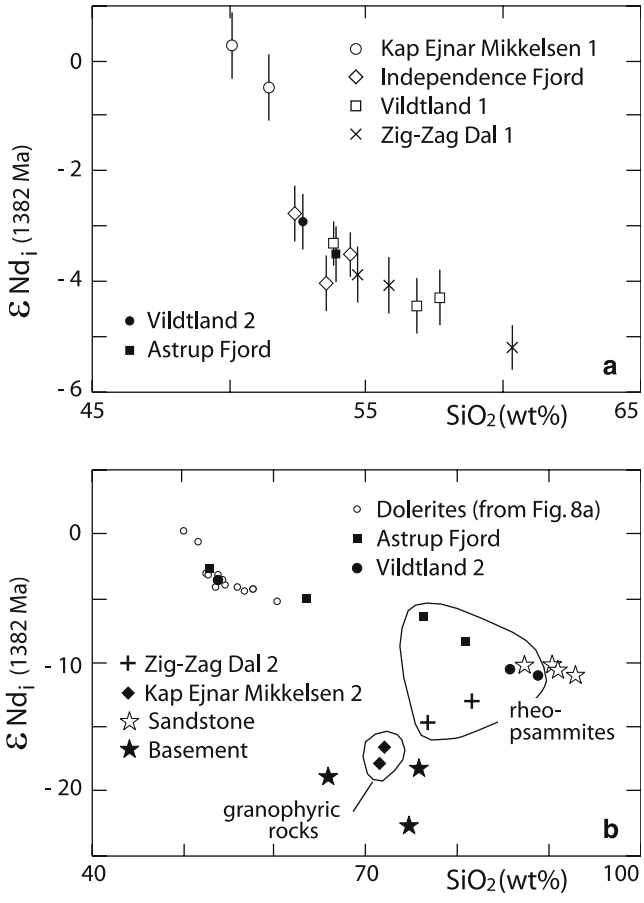

Fig. 8 εNd_i values (at 1,382 Ma) plotted against SiO_2. **a** doleritic rocks subdivided according to the different intrusions; **b** silicic rocks and dolerites [from (**a**); dolerites here shown with *small open circles*] compared to the sandstones and granitoid basement samples. Note covariation of εNd values with SiO_2 in the dolerites. SiO_2 recalculated on volatile-free base

Rb–Sr isotope data

New Sr isotope data (Table 4) were acquired for the 29 samples chosen for this study. Most of these had been analysed earlier by Kalsbeek and Jepsen (1983), and the old Rb/Sr ratios (XRF, calibrated with the help of USGS standards; Pankhurst and O'Nions 1973) were used for the calculation of $^{87}Rb/^{86}Sr$ values. Nine samples were newly analysed for $^{87}Rb/^{86}Sr$.

As noted earlier there is a major discrepancy between the 1,230 ± 20 Ma Rb–Sr whole-rock isochron age obtained by Kalsbeek and Jepsen (1983) on the red dolerite from Vildtland and the recently published U–Pb age of 1,382 ± 2 Ma on baddeleyite from the large dolerite sheet at Kap Ejnar Mikkelsen (Upton et al. 2005). Apart from the disagreement between the two age determinations, some of the old Rb–Sr isotope data were incompatible with an age of 1,382 Ma, in that they yielded unrealistically low initial $^{87}Sr/^{86}Sr$ ratios (<0.7000) when calculated for that age. Three of the newly analysed samples also yielded initial $^{87}Sr/^{86}Sr$ ratios <0.7000, even when calculated for an age of 1,230 Ma. All samples with such low calculated initial $^{87}Sr/^{86}Sr$ represent hydrothermally altered rocks; one is the sandstone #273260 mentioned earlier.

In order to exclude the possibility that these features were due to errors in the old Rb–Sr isotope data, eight more samples from the red dolerite of Vildtland 1 were reanalysed for $^{87}Rb/^{86}Sr$ and $^{87}Sr/^{86}Sr$ (Table 4). The new data yielded an errorchron with a slope corresponding to an age of 1,245 ± 35 Ma (MSWD 3.09), similar to the earlier result (Fig. 9a). To further test the accuracy of the Rb/Sr analyses (used to calculate $^{87}Rb/^{86}Sr$ ratios) a comparison was made between data from Kalsbeek and Jepsen (1984) on the Zig-Zag Dal basalts and new analytical data on the same samples by J.G. Fitton and D. James (Upton et al. 2005, and unpublished data). The two data sets are in close agreement (within 1% for most samples; Fig. 9b). In summary, the inconsistencies noted above are not due to analytical errors but require a geological explanation. This is further discussed in a later section.

Pb–Pb isotope data

Pb isotope data (Table 5) for the different intrusions scatter about a 1,382 Ma reference isochron with model μ_1 8.0 in a $^{207}Pb/^{204}Pb$ vs. $^{206}Pb/^{204}Pb$ diagram (Fig. 10a, b). Surprisingly, there is no clear distinction in Pb-isotopic compositions between the dolerites and the granophyric and rheopsammitic rocks. Samples from the crystalline basement plot far above the 1,382 Ma reference isochron; this is not reflected in the Pb-isotopic compositions of the two granophyric samples from Kap Ejnar Mikkelsen 2. Three sandstone samples have somewhat lower $^{206}Pb/^{204}Pb$ than the intrusive rocks, while sample #273260 (the hydrothermally altered sandstone) has higher $^{206}Pb/^{204}Pb$.

The two dolerite samples from Kap Ejnar Mikkelsen 1 are distinct from the other samples in having somewhat lower $^{207}Pb/^{204}Pb$ at similar $^{206}Pb/^{204}Pb$; these samples also exhibit differences from the other dolerites in Sm–Nd and Rb–Sr relationships (see above).

In $^{208}Pb/^{204}Pb$ vs. $^{206}Pb/^{204}Pb$ diagrams (Fig. 10c, d) the dolerites plot along a well-defined trend line with a slope of ~1, consistent with an overall Th/U ratio of ~3.5 for the various samples, in good agreement with Th/U ratios found by ICP-MS analysis (Table 2). The silicic rocks define a slightly steeper trend, compatible with a Th/U ratio of ~4.0 for the source of these rocks. This is slightly lower than the present-day Th/U ratios (4.0–5.1) of the analysed samples.

Discussion

Origins of the silicic intrusions

Based on similarities in major element compositions, Kalsbeek and Jepsen (1983) interpreted the granophyric

Table 4 Rb–Sr isotope data

Sample no.	Rb, ppm (ICP-MS)	Sr, ppm (ICP-MS)	$^{87}Rb/^{86}Sr$ (XRF)	$^{87}Sr/^{86}Sr$	$\pm 2\sigma$ (ppm)	$^{87}Sr/^{86}Sr_i$ 1,382 Ma	$^{87}Sr/^{86}Sr_i$ 1,230 Ma
Kap Ejnar Mikkelsen 1							
273241	8.0	151	0.165	0.705962	19	0.7027 ± 0.0001	0.7031
273247	4.9	177	0.083	0.705100	8	0.7035 ± 0.000	0.7036
Independence Fjord							
273228	42	222	0.557	0.714996	10	0.7040 ± 0.0002	0.7052
273230	58	196	0.857	0.726938	11	0.7100 ± 0.0003	0.7118
273236	66	60	3.121	0.745814	8	**0.6840 (!)** ± 0.0012	**0.6908 (!)**
Vildtland 1							
273390	27	171	0.443	0.713409	9	0.7046 ± 0.0002	0.7056
273391	87	237	1.072	0.731754	8	0.7105 ± 0.0004	0.7129
273392	69	155	1.294	0.734882	9	0.7092 ± 0.0005	0.7121
273393	77	123	1.831	0.746417	7	0.7101 ± 0.0007	0.7142
273395	61	72	2.464	0.756145	7	0.7073 ± 0.0010	0.7127
273396	62	69	2.643	0.760077	14	0.7077 ± 0.0011	0.7135
273397	57	76	2.190	0.751755	13	0.7084 ± 0.0009	0.7132
273398	72	56	3.666	0.778814	7	0.7062 ± 0.0015	0.7142
273399	68	71	2.794	0.763068	6	0.7077 ± 0.0011	0.7138
273400	80	41	5.705	0.812716	8	**0.6997 (!)** ± 0.0023	0.7122
273401	79	45	5.136	0.803760	7	0.7020 ± 0.0020	0.7133
Zig-Zag Dal 1							
273482	37	173	0.636	0.717782	9	0.7052 ± 0.0003	0.7066
273487	44	153	0.818	0.722804	8	0.7066 ± 0.0003	0.7084
273495	79	139	1.620	0.741787	8	0.7097 ± 0.0006	0.7132
Kap Ejnar Mikkelsen 2							
273214	109	101	3.004	0.774431	7	0.7149 ± 0.0012	0.7215
273219	114	74	4.253	0.797163	10	0.7129 ± 0.0017	0.7222
Astrup Fjord							
197402	29	150	0.564	0.715019	9	0.7038 ± 0.0002	0.7051
197405	135	78	4.947	0.808788	9	0.7107 ± 0.0020	0.7216
197406	88	18.4	13.64	0.957452	42	**0.6871 (!)** ± 0.0054	0.7172
197408	85	10.6	22.17	1.058134	6	**0.6188 (!)** ± 0.0088	**0.6675 (!)**
Vildtland 2							
273364	38	147	0.742	0.719673	12	0.7050 ± 0.0003	0.7066
273367	80	18.1	12.16	0.954166	7	0.7132 ± 0.0048	0.7399
273370	86	19.7	12.40	0.945185	7	**0.6994 (!)** ± 0.0049	0.7267
Zig-Zag Dal 2							
273525	101	55	5.26	0.825959	8	0.7218 ± 0.0021	0.7333
273532	120	34	10.18	0.908567	9	0.7068 ± 0.0040	0.7292
Crystalline basement							
197429	130	507	0.665	0.729834	9	0.7167 ± 0.0003	0.7181
197439	246	106	6.57	0.894291	9	0.7641 ± 0.0026	0.7785
197440	285	84	9.53	1.019656	7	0.8307 ± 0.0038	0.8517
Sandstones							
273260	47	6.7	20.41	1.058071	8	**0.6536 (!)** ± 0.0081	**0.6985 (!)**
273262	135	40	9.21	0.936033	16	0.7534 ± 0.0037	0.7737
273293	106	32	9.68	0.937012	7	0.7452 ± 0.0038	0.7665
273402	109	31	10.06	0.957655	7	0.7583 ± 0.0040	0.7804

Analysed at the Geological Institute, University of Copenhagen. Initial $^{87}Sr/^{86}Sr$ ratios for ages of 1,382 and 1,230 Ma were calculated assuming closed-system behaviour of the Rb–Sr isotope relationships after 1,382 and 1,230 Ma, respectively. Some of the samples yield unrealistically low initial $^{87}Sr/^{86}Sr$ ratios (bold numbers with !). Precisions (2σ) of Sr_{1382} values are based on 2σ errors on $^{87}Rb/^{86}Sr$ ratios of 2%; errors on Sr_{1230} values are slightly lower than those of the former

rocks of Kap Ejnar Mikkelsen 2 to represent melted crystalline basement, and the rheopsammites from Vildtland 2 and Astrup Fjord to be mobilised sandstones. Nd isotope data (Table 3) support these interpretations. The granophyric rocks have εNd_i values (at 1,382 Ma) similar to those of basement samples, and the rheopsammites of Vildtland 2 have εNd_i similar to the sandstones (Fig. 8b). The rheopsammitic samples from Astrup Fjord have εNd_i and SiO_2 intermediate between sandstones and dolerites, supporting the view that they contain components derived from these two sources (cf. Figs. 3, 4), and the two samples from Zig-Zag Dal 2 have εNd_i and SiO_2 intermediate between sandstone and basement samples, consistent with the view that they may contain components of both, as suggested by the major element data (Fig. 4).

Trace element data further support the crustal origin of the silicic rocks. REE spectra for the granophyric rocks of Kap Ejnar Mikkelsen 2, with high LREE and low HREE, are broadly similar to those of some

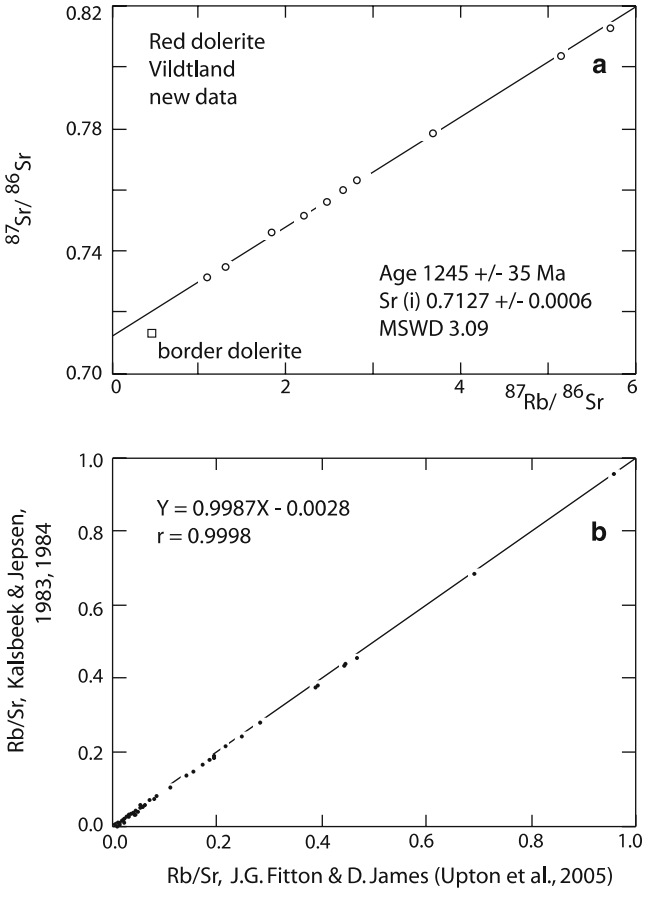

Fig. 9 **a** Rb–Sr whole-rock isochron diagram for the 'red' dolerite from Vildtland, reanalysed for this study. The samples fall along a well-defined errorchron suggesting an age of ~1,245 Ma, which is not the true age of the rocks; see text. **b** Comparison of Rb/Sr ratios (X-ray fluorescence spectrometry; used to calculate $^{87}Rb/^{86}Sr$ ratios) obtained for samples from the Zig-Zag Dal basalts and Midsommersø dolerites by Kalsbeek and Jepsen (1983, 1984) compared to results of J.G. Fitton and D. James (Upton et al. 2005, and unpublished data) on the same samples

basement samples (Fig. 6), and rheopsammitic rocks from Astrup Fjord and Vildtland 2 have low REE and distinct negative Eu anomalies, similar to sandstone samples. In the spider diagrams (Fig. 7), the granophyric rocks and the rheopsammites display pronounced negative anomalies for Nb, Sr, P and Ti, similar to basement and sandstone samples, and dissimilar to most of the dolerites in which these anomalies are smaller.

Rocks similar to the North Greenland rheopsammites are rare. Although most continental flood basalt provinces have associated dolerite dykes and sills, commonly emplaced into sandstones, rheopsammites have not been reported—see e.g., Cox (1988) and Marsh et al. (1997) on the Karroo Province, Peate (1997) on the Paraná-Etendeka Province, and Saunders et al. (1997) on the Tertiary North Atlantic Province. Obviously in North Greenland basic magma reacted with the crystalline basement and the sandstones at depth under conditions that are not commonly realised. This topic is treated in a later section.

Crustal contamination of the dolerites

All the investigated dolerites have negative anomalies for Nb, Sr, P and, with the exception of Kap Ejnar Mikkelsen 1, for Ti in the spider diagrams (Fig. 7). For the samples from Kap Ejnar Mikkelsen 1 the anomalies are small, for all other dolerites they are quite distinct. Further, all dolerites, except those of Kap Ejnar Mikkelsen 1, have negative εNd_i values at 1,382 Ma (Fig. 8). These features are consistent with crustal contamination of a mantle-derived magma, but they could also be caused by an origin of the magmas from an enriched lithospheric mantle, or by interaction of basic magma with such enriched mantle (e.g. Patchett et al. 1994). In fact, Upton et al. (2005) suggest that interaction with enriched lithospheric mantle was the major cause of the low εNd_i values (−2 to −4) in the Basal and Aphyric units of the Zig-Zag Dal basalts.

The investigated dolerites have 50–63% SiO_2 (volatile-free), and there are systematic correlations between such parameters as La_N/Sm_N (the steepness of the LREE spectrum) and the magnitude of the negative Nb, Eu (and Ti) anomalies in the spider diagrams with increasing SiO_2 (Fig. 11). The same feature was noted above for the εNd_i values (Fig. 8). In all cases the compositions of the SiO_2-enriched dolerites plot along mixing lines towards the compositions of the granophyric and rheopsammitic rocks. Since dolerites with variable SiO_2 commonly occur within one and the same intrusion (e.g. Vildtland 1, Zig-Zag Dal 1, Astrup Fjord) these systematic variations cannot be the results of variable mantle sources or variable interaction with lithospheric mantle, and must be a consequence of crustal contamination.

Chemical effects of hydrothermal alteration

Hydrothermally altered rocks have markedly higher K_2O and Rb and lower CaO, Sr and Ba than unaltered equivalents. Na_2O behaves more erratically with both higher and lower Na_2O in altered than in unaltered dolerites. For the red dolerites of Vildtland 1 and the granophyric rocks of Kap Ejnar Mikkelsen 2 concentrations of K_2O and Na_2O show statistically significant negative correlations (Kalsbeek and Jepsen 1983). High Pb in a few hydrothermally altered dolerite chills (e.g. 47 ppm in #273236, compared to 1–12 ppm in other dolerites; Table 2) demonstrates mobility of Pb. This is confirmed by the Pb-isotopic data (see below).

Most other elements appear little affected by the hydrothermal alteration. REE patterns for the different dolerites, altered and unaltered, are very similar (Fig. 6). The same appears true for other elements that are generally considered to be immobile during weathering and

Table 5 Pb isotope data

Sample	$^{206}Pb/^{204}Pb$	$\pm 2\sigma$	$^{207}Pb/^{204}Pb$	$\pm 2\sigma$	$^{208}Pb/^{204}Pb$	$\pm 2\sigma$	ρ_1	ρ_2
Kap Ejnar Mikkelsen 1								
273241	17.695	0.022	15.436	0.021	37.647	0.053	0.977	0.958
273247	17.717	0.013	15.412	0.013	37.901	0.036	0.958	0.929
Independence Fjord								
273228	17.958	0.016	15.474	0.015	37.858	0.041	0.968	0.940
273230	17.317	0.015	15.433	0.015	37.064	0.039	0.967	0.950
273236	16.847	0.013	15.434	0.013	36.737	0.035	0.958	0.921
Vildtland 1								
273390	17.939	0.014	15.511	0.014	37.933	0.038	0.970	0.934
273392	17.790	0.015	15.487	0.015	37.632	0.040	0.956	0.923
273398	18.004	0.020	15.497	0.010	37.942	0.048	0.978	0.960
Zig-Zag Dal 1								
273482	19.026	0.017	15.584	0.015	38.993	0.042	0.975	0.946
273487	18.479	0.015	15.533	0.014	38.408	0.038	0.966	0.938
273495	17.579	0.013	15.459	0.013	37.601	0.035	0.967	0.940
Kap Ejnar Mikkelsen 2								
273214	17.516	0.011	15.471	0.012	37.530	0.033	0.966	0.934
273219	18.287	0.016	15.533	0.015	38.713	0.040	0.970	0.944
Astrup Fjord								
197402	17.166	0.013	15.431	0.013	37.064	0.035	0.958	0.929
197405	16.873	0.011	15.410	0.012	36.743	0.032	0.960	0.929
197406	16.995	0.010	15.403	0.011	36.960	0.030	0.967	0.933
197408	18.017	0.014	15.462	0.014	38.113	0.038	0.962	0.926
Vildtland 2								
273364	18.579	0.016	15.533	0.015	38.609	0.041	0.967	0.948
273367	19.064	0.020	15.566	0.018	38.805	0.047	0.975	0.956
273370	20.231	0.023	15.639	0.019	40.384	0.051	0.975	0.958
Zig-Zag Dal 2								
273525	18.416	0.015	15.585	0.014	38.621	0.039	0.948	0.924
273532	18.957	0.022	15.591	0.020	40.267	0.053	0.975	0.963
Crystalline basement								
197429	19.748	0.010	16.051	0.010	43.856	0.033	0.956	0.933
197432	26.927	0.018	16.672	0.013	39.422	0.034	0.961	0.930
197440	20.646	0.013	16.184	0.012	42.679	0.037	0.960	0.932
Sandstones								
273260	19.441	0.018	15.628	0.016	39.990	0.044	0.969	0.938
273262	15.997	0.010	15.262	0.012	35.824	0.032	0.943	0.922
273293	16.150	0.011	15.298	0.012	35.994	0.033	0.973	0.937
273402	16.071	0.013	15.255	0.014	36.142	0.037	0.968	0.934

Analysed at the Geological Institute, University of Copenhagen; ρ_1, ρ_2 correlation coefficients after Ludvig (2003)

alteration (e.g. Ti, Zr, Nb; Fig. 7). Some mobility of SiO_2 during alteration cannot be excluded, but high SiO_2 in some of the altered samples cannot be due to mobility of SiO_2 alone because of the correlation of SiO_2 with such parameters as εNd_i and La_N/Sm_N noted above.

Sr isotope data and the 1,230 Ma Rb–Sr isochron date

As noted above, Rb–Sr isotope data yield internally inconsistent results in that initial $^{87}Sr/^{86}Sr$ ratios calculated for ages of 1,382 (and 1,230) Ma for some of the hydrothermally altered samples are <0.7000. We demonstrated earlier that this is not due to analytical errors, and a geological explanation is therefore required.

We suggest that the hydrothermally altered rocks have not been closed with respect to Sr after the end of the hydrothermal event, and that later loss of Sr increased their $^{87}Rb/^{86}Sr$ ratios. Since the intrusions have not suffered deformation or metamorphism subsequent to their emplacement, it is plausible that this Sr loss is related to recent surface weathering. In these hydrothermally altered rocks most or all feldspar has been replaced by secondary minerals, within which Sr is apparently poorly bound. It would seem that some Sr goes into solution during surface exposure and is removed, even from fresh-looking rocks. This feature is well known for U (e.g. Rosholt et al. 1973), but has not, to our knowledge, been reported earlier for Sr. Accepting that the $^{87}Rb/^{86}Sr$ ratios of hydrothermally altered samples have been increased by late loss of Sr means that the 1,230 Ma isochron age obtained by Kalsbeek and Jepsen (1983) does not have geological significance. The reasonable fit of the data points on the new errorchron line (Fig. 9a) must then be largely accidental.

The earlier Rb–Sr isotope data led to the following conclusions (Kalsbeek and Jepsen 1983): The lowest initial $^{87}Sr/^{86}Sr$ ratios (Sr_i), 0.7029–0.7038 at 1,230 Ma (slightly lower at 1,382 Ma; Table 4), were obtained for the dolerites of Kap Ejnar Mikkelsen 1. Most other

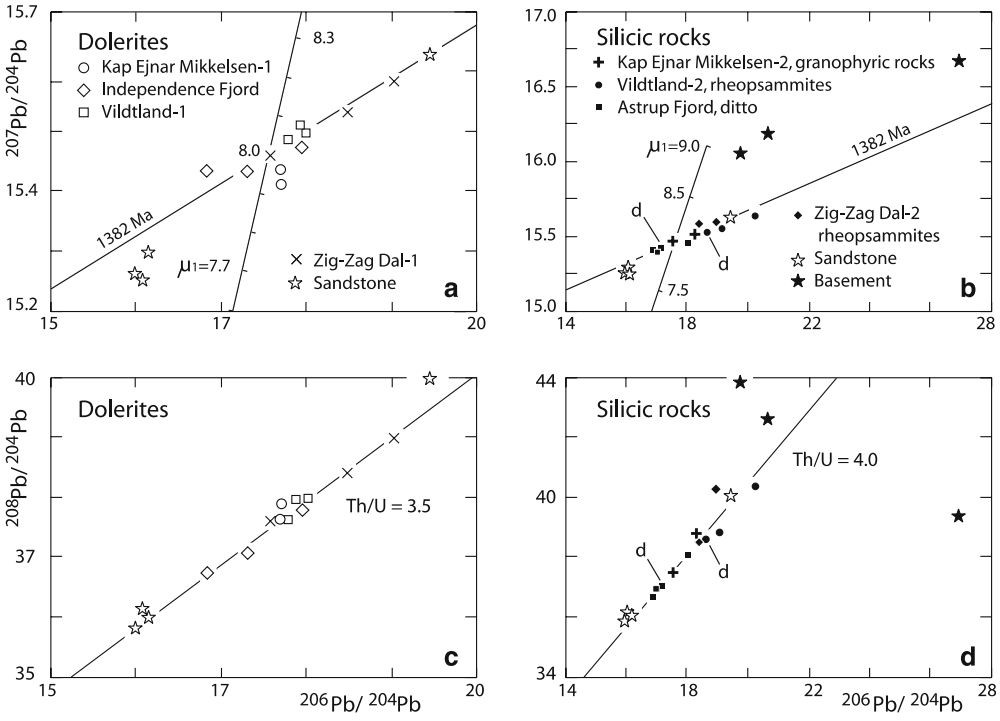

Fig. 10 $^{207}Pb/^{204}Pb$ and $^{208}Pb/^{204}Pb$ vs. $^{206}Pb/^{204}Pb$ diagrams. **a** and **c** doleritic intrusions; **b** and **d** silicic intrusions compared to the sandstones and granitoid basement samples. Samples marked *d* are the dolerite borders of the rheopsammitic intrusions. Note the marked difference in Pb-isotopic compositions of the granophyric rocks from Kap Ejnar Mikkelsen 2 and samples of the granitoid basement by melting of which they are believed to have been formed. For discussion see the text

'grey' dolerites had Sr_i 0.705–0.709, whereas 'red' (hydrothermally altered) dolerites had slightly higher Sr_i values, 0.710–0.713. The granophyric rocks from Kap Ejnar Mikkelsen 2 had $Sr_i \sim 0.719$, lower than basement samples, and the rheopsammites from Vildtland 2 and Zig-Zag Dal 2 had $Sr_i \sim 0.730$, lower than the sandstones. It was inferred that the Sr in the red dolerites and the crustally derived intrusions is a mixture of Sr from the dolerites and Sr from the surrounding sandstones introduced during hydrothermal alteration (perhaps with a component derived from the crystalline basement). In view of the problems with the $^{87}Rb/^{86}Sr$ ratios described above, and since the dolerites have been shown to be older than assumed previously (Upton et al. 2005), these results must be viewed with reservation. However, since the measured $^{87}Rb/^{86}Sr$ ratios overestimate the original values, the true Sr_i values must be higher than those calculated, and it is therefore likely that the earlier conclusions remain broadly correct.

Pb isotopes

The scatter of the Pb-isotopic data points along a 1,382 Ma reference isochron in the $^{207}Pb/^{204}Pb$ vs. $^{206}Pb/^{204}Pb$ diagram (Fig. 10a) suggests that there may not have been major Pb-isotopic differences between the different intrusive rocks 1,382 Ma ago. Surprisingly, the granophyric rocks have Pb-isotopic compositions totally different from the granitoid basement by melting of which they are believed to have been formed. We suggest that the present Pb-isotopic compositions of these rocks are mainly the results of the hydrothermal alteration of the rocks, and to a much lesser extent reflect their magmatic origins.

Generation and emplacement of rheopsammitic magma

From the lack of rheopsammitic rocks in other flood basalt provinces it may be concluded that in North Greenland basic magma reacted with the sandstones at depth under conditions that are not commonly realised. We consider that the magma intruded as major sheets at or near the boundary of the basement with the sandstones, as well as within the sandstones. The large proportion of dolerite relative to sandstone commonly observed in the field (Fig. 1) apparently led to partial melting at depth, and with some 25% K-feldspar, enough eutectic melt could be formed in the sandstones to mobilise the rock. The presence of pore water in the sandstones would promote melting. Thermal conditions for this process are considered below.

Eutectic melting of water-saturated quartz–K-feldspar mixtures takes place at ~800°C at a pressure of 1 kb and ~750°C at 2 kb (Bohlen et al. 1983; Johannes and Holtz 1996). With an estimated thickness of ~2 km for the Independence Fjord Group (Collinson 1983) and ~1 km of overlying basalts rheopsammite formation may have taken place at pressures as low as ~1 kb. However, the thicknesses of both the sandstone succession (the base of which is not exposed) and the basalts (the top of which has been removed by erosion) are poorly constrained, and the presence of dolerite intrusions within the sandstones (> 1 km) must be taken into consideration. Nevertheless, it is improbable that

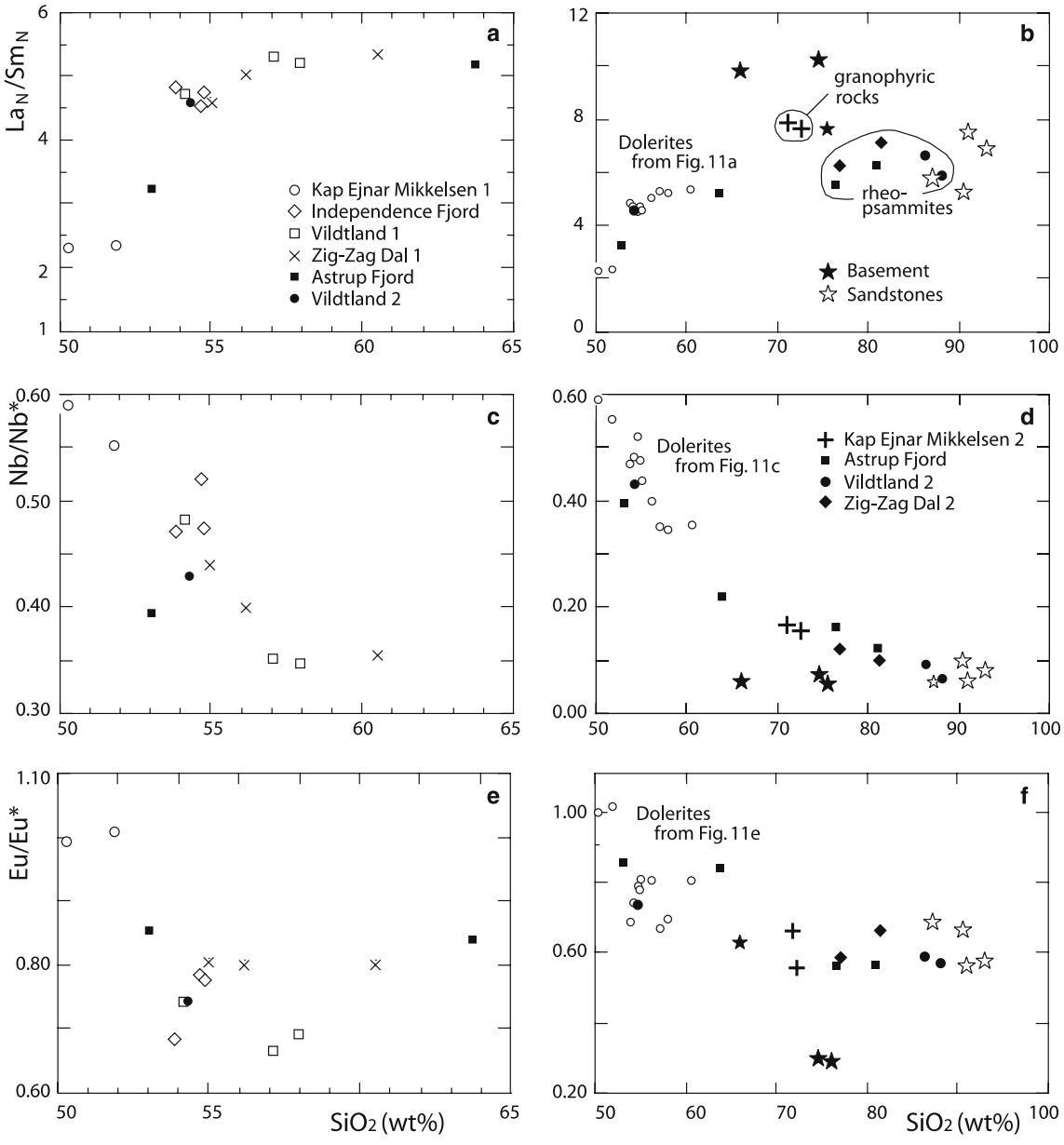

Fig. 11 Plots of La_N/Sm_N, Nb/Nb* and Eu/Eu* against SiO_2. **a**, **c** and **e** doleritic rocks subdivided according to the different intrusions; **b**, **d** and **f** silicic rocks and dolerites [from (**a**), (**c**) and (**e**); dolerites here shown with *small open circles*] compared to the sandstones and granitoid basement samples. Note covariation of La_N/Sm_N, Nb/Nb* and Eu/Eu* with SiO_2 in the dolerites. Nb* calculated by interpolation between Th and La in the chondrite-normalised spider diagrams. SiO_2 recalculated on volatile-free base

pressures much higher than 2 kb were attained, and rheopsammite formation must therefore have taken place at temperatures of at least ~750–800°C. The common occurrence of quartz as pseudomorphs after tridymite (Fig. 3), however, suggests significantly higher temperatures.

The thermal effects of solidifying intrusions on their country rock can be evaluated using heat conduction equations discussed by, e.g. Jaeger (1964), Delaney (1987), and Turcotte and Schubert (2002). Figure 12 shows peak temperatures attained within sandstone near the border of a solidifying dolerite sill at 1,100°C, and country rock temperatures (T_0) of 100, 300, 500 and 700°C (curves 1–4), modelled using equations from Turcotte and Schubert (2002). The thickness of the sill has no influence on the shape of the temperature profiles, but the width of the thermal aureoles are directly proportional to the sill thickness. The time of solidification (t_s) is proportional to the square of the sill thickness; t_s values shown in Fig. 12 were calculated for a dyke thickness of 100 m. Curves a, b and c in Fig. 12 show the temperatures attained within a screen of sandstone enclosed between two equally thick dolerite sills, assuming the sandstone has a width of 100% (a), 70% (b) and 50% (c) of the sill thickness, and T_0 = 100°C.

It is immediately apparent from the diagram of Fig. 12 that partial melting in the sandstones near the contact with a single dolerite sill could only take place if T_0 was already elevated before sill intrusion. With a thermal gradient of 25°C km^{-1} T_0 would be ~100°C; the temperature at the dolerite contact (T_c) would be ~690°C, and melting would not take place. With T_0 = 300°C and the corresponding T_c = ~ 780°C, local melting might be possible, but only over a small interval, since the temperature gradient is steep near the dolerite contact. Only at high T_0 values would significant volumes of rheopsammitic magma be expected to be formed. Moreover, at high T_0 the temperature gradients at the dolerite contact would be much shallower, consistent with the absence of sharp, chilled contacts between doleritic and rheopsammitic rocks.

In case of sandstone heated from two sides by two solidifying dolerites (Fig. 12, curves a, b, c), assuming T_0 = 100°C, melting would only take place if the sandstone was significantly thinner than the two dolerite sills. For example, a 70-m sandstone screen, between two dolerites of 100 m each, would hardly get hotter than ~700°C over most of its width (curve b), but a layer of sandstone of 50 m would be heated to > 800°C (curve c). Also in this case the shallow thermal gradient at the dolerite–sandstone contact would be consistent with the absence of chilled contacts between sandstones and dolerites.

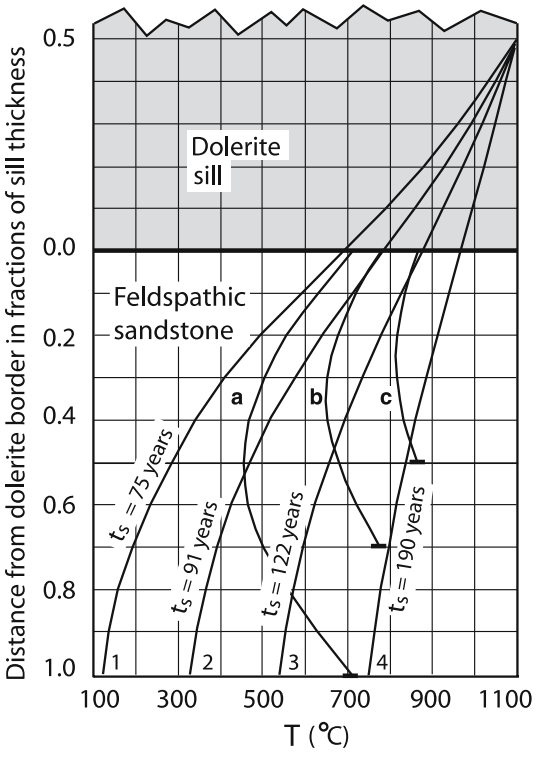

Fig. 12 Peak temperature profiles in sandstone near the margins of solidifying dolerite sills, calculated using equations and parameters for thermal conductivity from Turcotte and Schubert (2002); L (latent heat) = 320 kJ kg^{-1}, c (specific heat) = 1.2 kJ kg^{-1} K^{-1} and κ (thermal diffusivity) = 0.5 mm^2 s^{-1} . Distances from the dolerite–sandstone contact are given as fractions of sill thickness. Curves 1–4 show maximum temperatures attained in the sandstones assuming a dolerite temperature of 1,100°C and initial country rock temperatures (T_0) of 100, 300, 500 and 700°C, respectively. The time needed for dolerite solidification (t_s) is proportional to the square of the sill thickness; t_s values shown in the figure were calculated for a sill thickness of 100 m. Curves a, b and c show peak temperatures within a layer of sandstone between two equally thick solidifying dolerites, where the width of the sandstone is 100, 70 and 50% of the thickness of the dolerites. See text for discussion

Possible cooling by circulating fluids and heating by continued magma flow through the sills (e.g. Delaney 1987) are not considered in this model which, therefore, must be regarded as an approximation only. Nevertheless, the model indicates that the generation of rheopsammitic magma requires either (1) that large proportions of hot basic magma heated the country rocks to such high temperatures, that continued influx of magma could lead to extensive melting within the sandstones, or else (2) that screens of sandstone were caught between thick dolerite sills. Since solidification of dolerite sills takes place over relatively short periods (a few hundreds to perhaps 1,000 years for sills 100–200 m thick) these dolerites must be emplaced within a short period of time. In both scenarios a high rate of dolerite emplacement is implied.

To explain the characteristic occurrence of rheopsammitic intrusions, invariably rimmed by dolerite (Fig. 2 in Kalsbeek and Jepsen 1983), we envisage a screen of hot sandstone entrapped between sheets of hot basic magma and partly melted (Fig. 13). Reaction between the basic and silicic melts, together with mixing of the different components, gives rise to a zoned magma chamber (Fig. 13a). Upward intrusion of melts from such a magma chamber would yield zoned intrusions, with outer margins stemming from the upper part of the chamber, followed by inner zones from deeper parts in the chamber, either 'red' SiO_2-enriched dolerite or rheopsammite (Fig. 13b).

Midsommersø dolerites and Zig-Zag Dal basalts

Upton et al. (2005) note a compositional overlap of the Midsommersø dolerites and Zig-Zag Dal lavas, especially those of the (lower) Aphyric unit. Our new data support and extend this result. Whereas the majority of the dolerites have moderately high La_N/Sm_N (Fig. 6), similar to the lavas of the Basal and Aphyric units, the dolerite of Kap Ejnar Mikkelsen 1 has low La_N/Sm_N, with REE patterns similar to those of lavas of the (upper) Porphyritic unit. In a Ce/Y vs. Zr/Nb diagram, employed by Upton et al. (2005) for their modelling of the petrogenesis of the Zig-Zag Dal basalts, the lavas from the Basal, Aphyric and Porphyritic units plot in distinct fields, with only little overlap. Unaltered dolerites with high LREE from Independence Fjord, Vildtland 1, Zig-Zag Dal 1 and the border dolerite from Vildtland 2 plot within or close to the fields of basalts from the Basal and Aphyric units (Fig. 13; the three

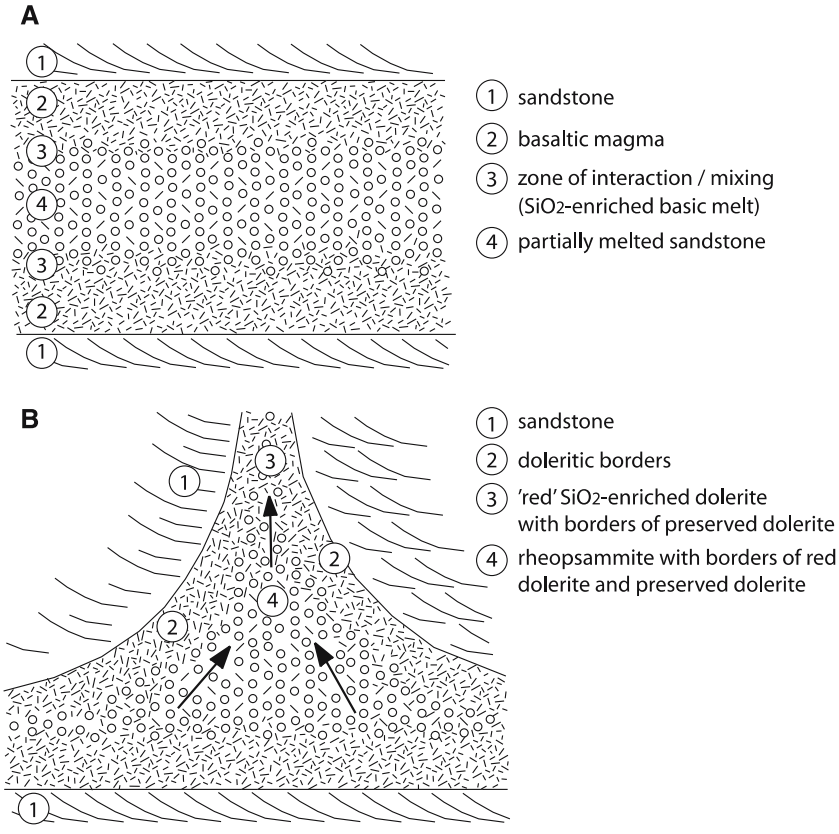

Fig. 13 Model to explain the presence of dark doleritic borders on both sides of intrusive sheets of 'red' SiO_2-enriched dolerite and rheopsammite. **a** Formation of a zoned magma chamber, from which zoned intrusions (**b**) are formed. See text for further explanation

samples at slightly higher Ce/Y are 'red' SiO_2-enriched dolerites), while the low-LREE dolerites from Kap Ejnar Mikkelsen 1 and the border dolerite from Astrup Fjord plot in the field of the Porphyritic basalts. Similarity of the dolerites from Kap Ejnar Mikkelsen 1 with the basalts of the Porphyritic unit is further expressed by high Fe and Ti in both compared to other dolerites and basalts (Kalsbeek and Jepsen 1983; Upton et al. 2005; Table 2). Chemical similarity of the dolerites of Kap Ejnar Mikkelsen 1 with the Porphyritic basalts, and the other dolerites with the lavas of the Basal and Aphyric units is further supported by the respective εNd_i values (at 1,382 Ma). These are around 0 for the dolerites of Kap Ejnar Mikkelsen, compared to mildly negative (−3 to −5) for the other dolerites (Table 3), similar to εNd_i values obtained, respectively, for the Porphyritic basalts and the lavas from the Basal and Aphyric units.

Since the Porphyritic lavas are stratigraphically younger than those of the Basal and Aphyric units, it appears that the dolerite at Kap Ejnar Mikkelsen (for which the age of 1,382 Ma was obtained) must also be younger than most other dolerites. The possibility that the old 1,230 Ma Rb–Sr isochron date could refer to a younger intrusive age for the red dolerite of Vildtland than that of the dolerite of Kap Ejnar Mikkelsen can therefore be rejected.

Although there is a close agreement in chemical (including Nd-isotopic) compositions between the intrusions and the lavas, there is one important difference: while most of the investigated dolerites have distinctly negative Eu anomalies (Fig. 6), such anomalies have not been observed for the lavas. The cause of this difference is enigmatic. To assure that the contrast is not due to interlaboratory differences, two of the basalts (#273405 and #273420) analysed by Upton et al. (2005) were reanalysed at GEUS. Our data were similar to those reported by Upton et al. (2005), and did not yield any Eu anomaly.

Eu anomalies in the dolerites are most probably related to crustal contamination (Fig. 11e, f). Since the basalts have passed through granitoid crust before eruption without acquiring negative Eu anomalies, it is possible that the Eu anomalies observed in most of the dolerites are mainly the result of interaction with the sandstones, not the crystalline basement rocks. It is not clear why the basalts were not similarly contaminated. Since no dykes have been observed within the Zig-Zag Dal basalts (and, indeed, hardly any dykes occur within the uppermost ~200 m of sandstones underlying the basalts), Upton et al. (2005, p. 42) suggested that the exposed lavas might be remote from their eruptive vents. It is therefore possible that the magmas that formed the lavas did not pass through the sandstones, thereby reducing the possibility of contamination.

Summary and conclusions

The Midsommersø dolerites and Zig-Zag Dal basalts of eastern North Greenland were formed during one

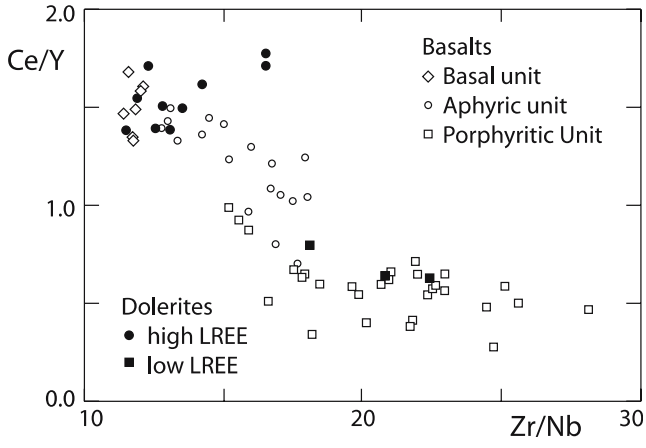

Fig. 14 Plot of Ce/Y vs. Zr/Nb comparing Zig-Zag Dal basalts and Midsommersø dolerites. This diagram was employed by Upton et al. (2005) to model the petrogenesis of the basalts. Lavas from the Basal, Aphyric and Porphyritic units plot in separate fields with very little overlap. Most Midsommersø dolerites have relatively high light rare earth element (LREE) and plot in the fields of the Basal and Aphyric basalts, whereas the low-LREE dolerites from Kap Ejnar Mikkelsen and Astrup Fjord fall in the field of the Porphyritic lavas. The three samples with high Ce/Y (relative to Zr/Nb) are 'red' SiO_2-enriched dolerites

igneous event around 1,380 Ma ago. An earlier reported age of 1,230 Ma (Kalsbeek and Jepsen 1983) has proved to be incorrect.

Silicic intrusions occur in association with the dolerites. They are the results of crustal melting due to the emplacement of large amounts of hot basic magma at high crustal levels within a short period of time. Some of these intrusions represent melted granitoid basement, while others have very high proportions of SiO_2 (up to ~90%) and were formed by partial melting and mobilisation of feldspathic sandstones which form the country rocks of the intrusions. Interaction of the basic magma with the sandstones and granitoid rocks from the basement gave rise to SiO_2-enriched (SiO_2 up to 63%) doleritic rocks.

All crustally derived rocks as well as the SiO_2-enriched dolerites have been affected by hydrothermal alteration, during which feldspar was largely or totally replaced by secondary minerals. The altered rocks are characterised by red colours, different from unaltered dolerites which are dark grey. During alteration the proportions of such elements as Na, K, Ca, Rb, Sr, Ba were strongly affected, while the concentrations of REE and other elements commonly regarded as less mobile (e.g. Ti, Zr and Nb) were not significantly changed.

Silicic intrusions and 'red' dolerites invariably have dark doleritic borders. This is interpreted to be the result of intrusion from zoned magma chambers within which screens of sandstone (or granitoid rocks) were partially melted and reacted with the basic magma.

Sr- and Pb-isotopic systems were strongly affected by the hydrothermal alteration and give little information on the petrogenesis of the rocks. Furthermore, recent loss of Sr from altered rocks during surface weathering has resulted in incompatible $^{87}Sr/^{86}Sr$ and $^{87}Sr/^{86}Sr$ ratios. Sm–Nd isotope systematics, however, were not affected by the alteration and support the inferences regarding the crustal origin of the silicic intrusions and the origin of the SiO_2-enriched dolerites by interaction between mantle-derived magma and crustal rocks.

There is a close compositional similarity between the Midsommersø dolerites and the Zig-Zag Dal basalts. However, most of the investigated dolerites have distinctly negative Eu anomalies, whereas such anomalies are not observed in the basalts. It is inferred that the Eu anomalies in the dolerites are due to contamination with components derived from crustal sources, mainly sandstones, but it is not clear why the basalts were not similarly contaminated.

Acknowledgments We thank the staffs of the laboratories involved in this study for their help. A.K. Higgins and Stefan Bernstein (both at GEUS) commented on drafts of the manuscript, and Benny Schark (GEUS) prepared Fig. 3. Comments from two anonymous reviewers and the editor were of great help during revision of the manuscript. Publication of this paper was authorised by GEUS.

Appendix: Sample descriptions; for further details see Kalsbeek and Jepsen (1983)

Kap Ejnar Mikkelsen 1. Near Kap Ejnar Mikkelsen (81°55.3′N–31°51.6′W) a 190-m thick horizontal sheet of very fresh dolerite crops out in the steep wall of Independence Fjord. For a detailed description and a chemical profile of this intrusion see Kalsbeek and Jepsen (1983). Sample nos. 273241 and 273247 were collected from the lower part of the sheet exposed in a large landslide, at respectively 40 and 85 m above the lower contact.

Independence Fjord. This intrusion at 81°54.9′N–32°05.3′W is a subhorizontal sheet of variable doleritic rocks, ~180 m thick. Apart from the bottom chill zone, the lower part of the intrusion is weathered to gravel; fresh rocks are present from 100 m upwards. Normal dolerites occur from 100 to 140 m, followed by red-and-greenish weathering granophyric dolerites. The upper 5 m consist of very fine-grained dark dolerite. Sample #273228 (+140 m) is a normal doleritic rock, #273230 (+160 m) a red granophyric dolerite, and #273236 represents the upper chill ~1 m below the contact with the sandstones. A chemical profile through the intrusion is shown in Kalsbeek and Jepsen (1983).

Vildtland 1. An isolated outcrop at 81°43.1′N–32°49.8′W exposes brick-red doleritic rocks. Contacts with the country rocks are not exposed, but there is a gradation of the red dolerite into normal dark-grey dolerite. The latter probably represents the border of the intrusion. Samples from this locality showed a wide range in Rb–Sr ratios, and yielded a Rb–Sr whole-rock isochron age of 1,230 ± 20 Ma. Three samples were selected for further study: #273390 represents the dark

border (?) dolerite; #273392 and #273398 are 'red dolerites'.

Zig-Zag Dal 1. At 80°56.6′N–26°19.9′W a thick (> 100 m; top not exposed) subhorizontal sheet of variable doleritic rocks crops out in a steep mountain side. At 80 m above the base there is, over an interval of some 2 m, a gradation from normal dark-grey dolerite to red doleritic rocks. Sample #273482 was collected from near the lower contact (+1.5 m), #273487 (+60 m) is a grey dolerite, and #273495 is a brick-red granophyric dolerite from higher up (> +100 m; precise height not known).

Kap Ejnar Mikkelsen 2. At 81°55.9′N–31°53.6′W a steeply inclined sheet of red granophyric rocks, with numerous inclusions of quartzite, occurs between a major dolerite and sandstones; contacts are not exposed. Samples #273214 and #273219 were chosen at random from a larger collection of very similar samples taken at this locality.

Astrup Fjord. A ~95 m thick, subhorizontal intrusive sheet is exposed within sandstone at 81°46.8′N–29°29.4′W, 10 km south of Astrup Fjord. It consists of 20 m dolerite at the bottom, followed by a thin zone (5 m) of granophyric dolerite, ~65 m of rheopsammite and, at the top, 5 m of dolerite. Contacts between the dolerites and the sandstones are sharp and chilled; all contacts within the intrusion are gradational over short distances. Sample #197402 represents the lower dolerite (5 m above the contact), #197405 is a red granophyric dolerite (+24 m), #197406 (+25 m) represents the transition between the red granophyric rock and the rheopsammites, and #197408 (+80 m) is a rheopsammite.

Vildtland 2. At 81°43.5′N–32°40.6′W a 25-m thick sheet of rheopsammitic rocks with doleritic borders is well exposed. The lower dolerite (5 m) is chilled against the sandstones and has a gradual transition over ~50 cm into rheopsammite. The upper dolerite is 1.5 m thick; it has a sharp chilled contact towards the sandstones and a narrow transitional contact with the central rheopsammites. Sample #273364 (+3 m) is a dolerite; #273367 (+10 m) and #273370 (+18 m) are typical rheopsammites. A chemical profile through the intrusion is shown in Kalsbeek and Jepsen (1983).

Zig-Zag Dal 2. At 80°57.1′N–26°17.5′W several flat-lying sheets of rheopsammite are rather poorly exposed in subhorizontal outcrops, and their geometry is therefore not well known. At least three separate intrusions, a few tens of metres across, and each with dark doleritic borders, are present. The two samples selected for this study, #273525 and #273532, come from two different intrusions.

Crystalline basement and sandstones. Three samples from basement rocks were taken from glacially transported boulders, which are scattered over the whole study area, and originate from underneath the Inland Ice. Representative sandstone samples were collected from various localities within the region.

References

Bohlen SR, Boettcher AL, Wall VJ, Clemens JD (1983) Stability of phlogopite–quartz and sanidine–quartz: a model for melting in the lower crust. Contrib Mineral Petrol 83:270–277

Collinson JD (1983) Sedimentology of unconformities within a fluvio-lacustrine sequence; Middle Proterozoic of eastern North Greenland. Sediment Geol 34:145–166

Cox KG (1988) The Karroo Province. In: MacDougall JD (ed) Continental flood basalts. Kluwer Academic Publishers, Dordrecht, pp 239–271

Delaney PT (1987) Heat transfer during emplacement and cooling of mafic dykes. In: Halls HC, Fahrig WF (eds) Mafic dyke swarms. Geological Association of Canada special paper 34, pp. 31–46

DePaolo DJ (1981) Neodymium isotopes in the Colorado Front Range and crust mantle evolution in the Proterozoic. Nature 291:193–196

Escher JC, Pulvertaft TCR (1995) Geological map of Greenland 1:2 500 000. Geological Survey of Greenland, Copenhagen

Govindaraju K (1994) 1994 compilation of working values and sample description for 383 geostandards. Geostand Newsl 18: 1–158

Jaeger JC (1964) Thermal effects of intrusions. Rev Geophys 2:433–466

Jepsen HF (1971) The Precambrian, Eocambrian and early Palaeozoic stratigraphy of the Jørgen Brønlund Fjord area, Peary Land, North Greenland. Medd om Grønland 192(2):1–42

Johannes W, Holtz F (1996) Petrogenesis and experimental petrology of granitic rocks. Springer, Berlin Heidelberg New York, 335 pp

Kalsbeek F, Jepsen HF (1983) The Midsommersø dolerites and associated intrusions in the Proterozoic platform of eastern North Greenland—a study of the interaction between intrusive basic magma and sialic crust. J Petrol 24:605–634

Kalsbeek F, Jepsen HF (1984) The late Proterozoic Zig-Zag Dal Basalt Formation in eastern North Greenland. J Petrol 25:644–664

Kystol J, Larsen LM (1999) Analytical procedures in the rock geochemical laboratory of the Geological Survey of Denmark and Greenland. Geol Greenland Surv Bull 184:59–62

Ludvig KR (2003) User's manual for ISOPLOT 3.00: a geochronological toolkit for Microsoft Excel. Berkeley Geochronology Center Special Publication 4, Berkeley, pp. 1–67

Marsh JS, Hooper PR, Rehacek J, Duncan RA, Duncan AR (1997) Stratigraphy and age of Karroo basalts of Lesotho and implications for correlations within the Karroo igneous province. In: Mahoney JJ, Coffin MF (eds) Large igneous provinces: continental, oceanic, and planetary flood volcanism. American Geophysical Union, Geophysical Monograph 100, Washington, pp. 247–272

Pankhurst RJ, O'Nions RK (1973) Determination of Rb/Sr and $^{87}Sr/^{86}Sr$ ratios of some standard rocks and evaluation of X-ray fluorescence spectrometry in Rb–Sr geochemistry. Chem Geol 12:127–136

Patchett PJ, Lehnert K, Rehkämper M, Sieber G (1994) Mantle and crustal effects on the geochemistry of proterozoic dikes and sills in Sweden. J Petrol 35:1095–1125

Peate DW (1997) The Paraná-Etendeka Province. In: Mahoney JJ, Coffin MF (eds) Large igneous provinces: continental, oceanic, and planetary flood volcanism. American Geophysical Union, Geophysical Monograph 100, Washington, pp. 217–245

Rosholt JN, Zartman RE, Nkomo IT (1973) Lead isotope systematics and uranium depletion in the Granite Mountains, Wyoming. Geol Soc Am Bull 84:989–1002

Saunders AD, Fitton JG, Kerr AC, Norry MJ, Kent RW (1997) In: Mahoney JJ, Coffin MF (eds) Large igneous provinces: continental, oceanic, and planetary flood volcanism. American Geophysical Union, Geophysical Monograph 100, Washington, pp. 45–93

Steiger RH, Jäger E (1977) Subcommission on geochronology: convention on the use of decay constants in geo- and cosmochronology. Earth Planet Sci Lett 36:359–362

Taylor SR, McLennan SM (1985) The continental crust: its composition and evolution. Blackwell, Oxford, 312 pp

Thompson RN (1982) British Tertiary volcanic province. Scott J Geol 18:49–107

Todt W, Cliff RA, Hanser A, Hofmann AW (1993) Re-calibration of NBS lead standards using a $^{202}Pb + ^{205}Pb$ double spike. Terra Abstr 5(Suppl. 1):396

Turcotte DL, Schubert G (2002) Geodynamics, 2nd edn. Cambridge University Press, Cambridge, 456 pp

Upton BGJ, Rämö OT, Heaman LM, Blichert-Toft J, Kalsbeek F, Barry TL, Jepsen HF (2005) The Mesoproterozoic Zig-Zag Dal basalts and associated intrusions of eastern North Greenland: mantle plume–lithosphere interaction. Contrib Mineral Petrol 149:40–56